CRYSTALLIZATION KINETICS OF TWO
METALLIC GLASSES BY MOSSBAUER
SPECTROSCOPY

Thesis

Denis E. Beller
AFIT/GNE/PH/81M-1 Captain   USAF
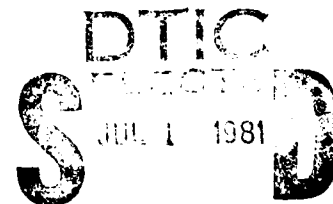
DTIC
ELECTED
JUL 1 1981

D

Approved for public release; distribution unlimited.

CRYSTALLIZATION KINETICS OF TWO METALLIC

GLASSES BY MOSSBAUER SPECTROSCOPY

THESIS

Presented to the Faculty of the School of Engineering of

of the Air Force Institute of Technology

Air University

In Partial Fulfillment of the

Requirements for the Degree of

Master of Science

by

Denis E. Beller, B.S.
Captain   USAF

Graduate Nuclear Engineering

March 1981

Preface

This thesis describes my efforts to determine the crystallization kinetics of two amorphous iron alloys, $Fe_{80}B_{20}$ and $Fe_{80}P_{6.5}C_{3.5}B_{10}$. The objectives of this study were: 1) to anneal the glasses at various temperatures, 2) to take Mossbauer spectra during the annealing, 3) to analyze the spectra to determine the growth of crystals, and 4) to use the crystallization rates to calculate the activation energy and projected lifetimes at 473 K. This thesis will summarize past work in this area, describe the equipment and methods, and present analysis of the Mossbauer spectra and the results, conclusions and recommendations.

I thank Dr. Harold Gegel of the Air Force Materials Laboratory for sponsoring this study and supplying the glassy metal ribbons. I especially thank my advisor, Dr. George John, for his continuous support and guidance. Finally, I am grateful to my wife, Judy, and my sons, David and Timothy, for their constant devotion and support during this long study.

Contents

iv

List of Figures

List of Tables

Abstract

In this study, Mossbauer spectroscopy was used to examine thermal aging of two metallic glasses. $Fe_{80}B_{20}$ was isothermally annealed at 573, 604, 611, and 626 K; and $Fe_{80}P_{6.5}C_{3.5}B_{10}$ was annealed at 614, 716, and 744 K. The activation energy of $Fe_{80}B_{20}$, determined from the growth of α-Fe crystals, was 0.256 ± 0.006 MJ/mole. The projected lifetime of this glass, based on the onset of crystallization, is 400 years. No quantitative data were obtained for $Fe_{80}P_{6.5}C_{3.5}B_{10}$; however, based on the higher temperature required for crystallization, it is expected to have a longer lifetime.

CRYSTALLIZATION KINETICS OF TWO METALLIC
GLASSES BY MOSSBAUER SPECTROSCOPY

I. Introduction

Mossbauer spectroscopy is becoming an increasingly important tool for studying the environments of nuclei. In this study, it was used to examine the crystallization characteristics of $Fe_{80}B_{20}$ and $Fe_{80}P_{6.5}C_{3.5}B_{10}$ amorphous alloys. These materials, commonly called metallic glasses, crystallize during accelerated aging at high temperatures.

Background

The glassy metals exhibit useful magnetic, as well as material (tensile strength, hardness, flexibility), properties.[1] The Air Force Materials Laboratory has become interested in their possible use in magnetic devices for Air Force weapons systems. As a result of this interest, in 1978 Schmidt (Ref 1) and Roberts (Ref 2) used Mossbauer spectroscopy to study the atomic structure of a few of the glassy metals, including $Fe_{80}B_{20}$. Because of projected high-temperature applications, the Materials Laboratory is concerned about thermal aging of these materials. Knowledge of the glasses' expected lifetimes at operating temperatures around 473 K is needed. predict the aging rates of these amorphous materials, one must know

---

[1]See Appendix E for a review of possible applications.

their crystallization characteristics. Many methods have been
used to determine these rates; all require measurements at 100
to 200 K above the expected operating temperature. In this
study, Mossbauer spectroscopy was used to examine the growth of
crystals in the metallic glasses $Fe_{80}B_{20}$ and $Fe_{80}P_{6.5}C_{3.5}B_{10}$.

Problem

The problem investigated in this study was to determine
the thermal aging rate of metallic glasses. Specifically, the
kinetics of crystallization of $Fe_{80}B_{20}$ and $Fe_{80}P_{6.5}C_{3.5}B_{10}$ were
studied. These glasses were examined by: 1) isothermal anneal-
ing, 2) taking Mossbauer spectroscopy during annealing, 3) eval-
uating the spectra to determine growth of α-Fe crystals, and 4)
using the crystallization rates at various temperatures to
determine the Arrhenius constant.

Scope

This study was limited to the investigation of only
two of the glassy metals, $Fe_{80}B_{20}$ and $Fe_{80}P_{6.5}C_{3.5}B_{10}$. The
temperature ranges were respectively 573 to 626 K and 716 to
744 K. The annealing periods were from one day at the high
temperatures to two weeks at the lowest temperatures. No
attempt was made to determine the structure of either the
amorphous or the crystalline material. In addition, the
literature studied was limited to only sources available at
the School of Engineering, Air Force Institute of Technology.

Review of the Literature

This section contains a review of some of the many
studies of the metallic glasses. These studies are mainly

cc...rned with three characteristics of the glasses: 1) amor-
phous structure, 2) temperature dependence of their magnetic
properties, and 3) thermal aging (or crystallization) charac-
teristics. Some of the results of these studies will be
presented in the discussion section in Chapter IV.

Luborsky studied the crystallization of $Fe_{80}B_{20}$,
$Fe_{40}Ni_{40}P_{14}B_6$, and $Fe_{40}Ni_{40}B_{20}$, using magnetic methods and
differential scanning calorimetry (Ref 3). Using the tempera-
ture of onset of crystallization at various heating rates, he
determined the activation energy for the three materials. He
also showed that thermal stability increased with the number
of atomic species, i.e., that $Fe_{80}B_{20}$ was the least stable of
the three glasses. Fukamichi and others studied the magneti-
zation, electrical resistivity, thermal expansion, and differ-
ential thermal change of a variety of Fe-B glasses (Ref 4).
They determined that the crystallization mechanism of the Fe-B
glasses depended on the concentration of boron. Chien studied
$Fe_{80}B_{20}$ from 4.2 K up to 1050 K, using Mossbauer spectroscopy,
and found that it crystallized to α-Fe and Fe_3B when annealed
at a high heating rate, but found only Fe_2B at low heating
rates (Ref 5). Luborsky and Lieberman examined the crystalli-
zation kinetics of the Fe-B glasses (12 to 28 percent boron)
by differential scanning calorimetry (Ref 6). They determined
that for 18 to 28 percent boron, the activation energy for
the onset of crystallization was independent of boron concen-
tration. However, Tarnoczi and others studied the role of
Fe_3B in the crystallization of Fe-B glasses, and concluded

3

that $Fe_{80}B_{20}$ was most stable (Ref 7). Matsuura, in a study similar to Luborsky and Lieberman's above, used differential thermal analysis on 12 to 20 percent boron Fe-B glasses (Ref 8). His results, obtained above 700 K, led to the conclusion that the formation of α-Fe accompanies the crystallization of Fe_3B. Chien and others did a lengthy study on Fe-B glasses (14 to 28 percent boron) and crystalline Fe_3B using Mossbauer spectroscopy and magnetization measurements (Ref 9). Kemeny and others used Mossbauer spectroscopy, differential scanning calorimetry, and magnetization measurements for a thorough investigation of the structure and crystallization of Fe-B metallic glasses (12 to 25 percent boron) (Ref 10). For 16 to 25 percent boron, they concluded that crystallization proceeds by the formation of α-Fe and Fe_3B in an eutectic process. They also deduced that the glass structure should be based on locally distorted, quasi-crystalline Fe_3B. Schaafsma and others have also done a lengthy crystallization study on two $Fe_{80}B_{20}$ glasses (Ref 11). They concluded that the crystallization mechanism did not change between 580 and 640 K. They also found that nucleation did not control the crystallization rate; i.e., that crystal nuclei exist in the as-quenched amorphous material. Finally, Kopcewicz used Mossbauer spectroscopy to study radio-frequency annealing of $Fe_{40}Ni_{40}B_{20}$ (Ref 12). He found that as a result of magnetostrictively induced atomic vibrations, a strong static rf field caused crystallization in LN_2- cooled samples.

Assumptions

The following were assumed to be true at the outset:

1) The $Fe_{80}B_{20}$ and $Fe_{80}P_{6.5}C_{3.5}B_{10}$ alloys were amorphous.

2) During annealing α-Fe and metastable Fe_3B were formed.

3) The compositions were true to within one percent.

Overview

The theory of the Mossbauer effect has been well documented and will not be presented here; however, the use of Mossbauer spectroscopy to study nuclear environments is presented in Chapter II, along with the theory of crystallization of Fe-B glasses. The Mossbauer equipment, annealing system, experimental procedures, and data processing are described in Chapter III. Chapter IV contains the results and discussion, and Chapter V contains the conclusions and recommendations.

II. Theory

The theory of the Mossbauer effect has been fully
developed and is well understood (see, e.g., Ref 13 and 14).
For a condensed and simplified explanation, see Roberts'
thesis (Ref·2: 3-11). Mossbauer spectroscopy measures the
hyperfine fields of nuclei. This is possible because the
hyperfine field interacts with the nuclear dipole moment,
which, for iron-57, splits the resonant-absorption energy
into six energy levels. The magnitudes of these energies are
directly proportional to the value of the hyperfine field,
which is characteristic of the electron environment of the
nucleus. Thus, for nuclei in a crystal, there are different
six-peak spectra (with Lorentzian line shapes) for each mag-
netically inequivalent site. For an amorphous material which
has only short-range order, there are very few magnetically
equivalent sites. The glass spectrum, then, is a combination
of many different six-peak spectra, with a probability dis-
tribution $P(H)$ describing the nuclear hyperfine fields. The
$P(H)$ of $Fe_{80}B_{20}$ have been described by Schmidt (Ref 1) and
Vincze (Ref 15) as a binomial distribution. This distribu-
tion was related to the number of nearest neighbors of iron
and non-iron nuclei. However, others have shown that the
glass spectra can be described by a model-independent pro-
bability distribution (Refs 15, 16, and 17). Schurer and

6

and Morrish have shown that a single six-line pattern, using Gaussian line shapes, describes the glass spectrum reasonably well (Ref 16: 819). This method is used in this study for the $Fe_{80}B_{20}$ glass.

When a metastable metallic glass is heated, it undergoes atomic rearrangement to a more stable, but still amorphous, state (Ref 18: 577). With further heating, it begins to crystallize. This crystallization has been described as a diffusion process, as one or more species migrates out of the amorphous region (Ref 11: 4428). For the Fe-B glasses, the possible crystalline states are α-Fe, FeB, Fe_2B, and Fe_3B. Fe_2B is expected to form during crystallization of the amorphous phase because it is much more stable than Fe_3B. For $Fe_{80}B_{20}$, however, the metastable Fe_3B (or $Fe_{75}B_{25}$) is much nearer the original composition than Fe_2B (or $Fe_{67}B_{33}$). Thus, others have found that α-Fe and Fe_3B are the species formed during annealing of $Fe_{80}B_{20}$ (Refs 7: 1026; 8:232; 10: 485; 11: 4429). While some determined that iron diffused from the glass to form α-Fe, leaving amorphous $Fe_{75}B_{25}$, which subsequently crystallized to Fe_3B (Ref 11: 4429), others deduced that Fe_3B crystallized accompanied by the simultaneous formation of α-Fe (Ref 8: 233). For a glass with many species, such as $Fe_{80}P_{6.5}C_{3.5}B_{10}$, there are many possible crystalline states. These include FeB, Fe_2B, Fe_3B, Fe_3C, Fe_3P, and combinations of these by atomic substitution, also with α-Fe.

The isothermal crystallization of an iron-based glass can be followed, then, by examining the growth of the six-peak

7

α-Fe spectrum in a series of Mossbauer spectra. The crystal-
line fraction x(t) is the ratio of the volume of α-Fe crystals
formed at time t to the volume in the fully crystallized
sample. It can be described by the Johnson-Mehl-Avrami
equation (Ref 11: 4426):

$$x(t) = 1 - \exp\left[-(k(T)t)^n\right] \qquad (1)$$

When rearranged, Eq (1) becomes

$$\ln \ln \frac{1}{1-x(t)} = n \ln k(T) + n \ln t \qquad (2)$$

which yields a straight line plot with slope n. Above, k(T)
is a temperature dependent constant, and the exponent n is
determined by the nucleation and growth characteristics of
the crystallization. The time $t_x(T)$ to crystallized fraction
x can be determined from Eq (2) for a series of isothermal
measurements. Then, for a thermally-activated diffusion
process, the Arrhenius equation describes the lifetime t_x
at constant x as a function of temperature T:

$$t_x = k_0^{-1} \exp\left(E_A/k_B T\right) \qquad (3)$$

where k_0 is a frequency factor, k_B is the Boltzman constant,
and E_A is the activation energy of the crystallization pro-
cess expressed as energy per atom (or per mole) (Ref 11: 4427).
Eq (3), when rearranged, also yields a straight line plot,
with slope E_A/k_B:

$$\ln t_x = \ln k_0^{-1} + (E_A/k_B)T^{-1} \qquad (4)$$

The above kinetic parameters can be derived from relatively quick measurements at high temperatures. If the assumption is valid that the crystallization process is the same over a large range of temperatures, then these constants can be used to predict the crystallization rate at lower temperatures. In this study, the crystallized fractions $x(t)$ were determined from the amplitudes of the α-Fe portions of Mossbauer spectra. The half lives $t_{.5}$ were then determined by least-squares curve fitting, and were used to determine the activation energy from the Arrhenius plot.

III.   Equipment and Procedures

In this section the Mossbauer spectroscopy equipment and annealing system are described. The procedures for preparing the glass samples and assembling them in the heater are included. Annealing the samples, taking the Mossbauer spectra during annealing, and analyzing the spectra are also described.

Mossbauer Equipment

The major Mossbauer spectroscopy components included a constant-acceleration velocity transducer (motor), a linear amplifier/single channel analyzer. a krypton-filled proportional counter, and a Mossbauer control unit (MCU). All were manufactured by Ranger Electronics. The Mossbauer spectrum was taken on an RIDL 400 multichannel analyzer (MCA), operated in the time-sequential scaling mode. With the exception of the time-base oscillator, which was an RIDL model 54-6, the equipment is the same as that described by Skluzacek (Ref 19: 5-11), Schmidt (Ref 1: 11-15), and Roberts (Ref 2: 12). The source, connected directly to the motor, was approximately 6 mCi cobalt-57 in a rhodium foil.

Annealing System

The annealing system consisted of a heater, a thermocouple reader, a vacuum system, and one of two temperature controllers. Ranger Engineering built the heater (Fig 1) as
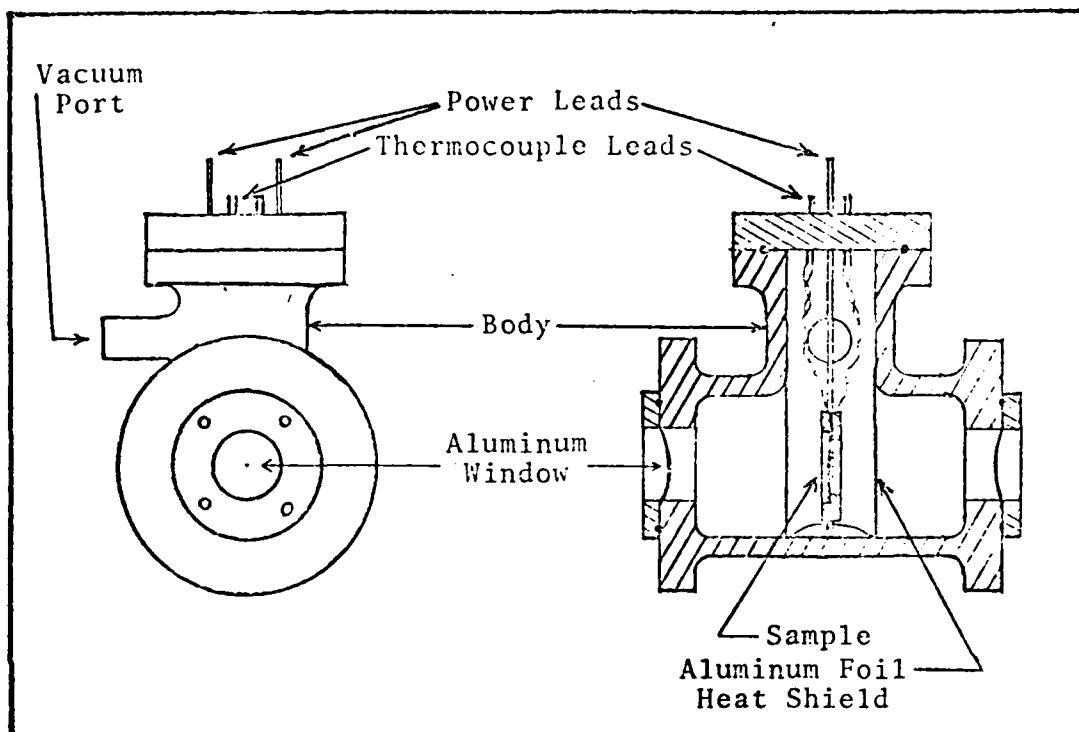
Fig 1. Heater (not to scale)

a prototype. The heating elements were two graphite discs
(0.135 ± 0.002 mm x 25.4 mm). The sample was held between the
heating discs and aligned with two aluminum foil windows
(0.025 ± 0.001 mm x 25.4 mm). There were two iron-constantan
thermocouples inside the heater; one was located in a slot at
the edge of the heating element frame, the other was centered
on the sample. The Omega thermocouple reader was calibrated
with ice, boiling water, and molten tin. The vacuum system
consisted of a forepump and an oil diffusion pump trapped with
liquid nitrogen. Its purpose was to prevent convection heat
transfer to the heater body. The first temperature controller,

11
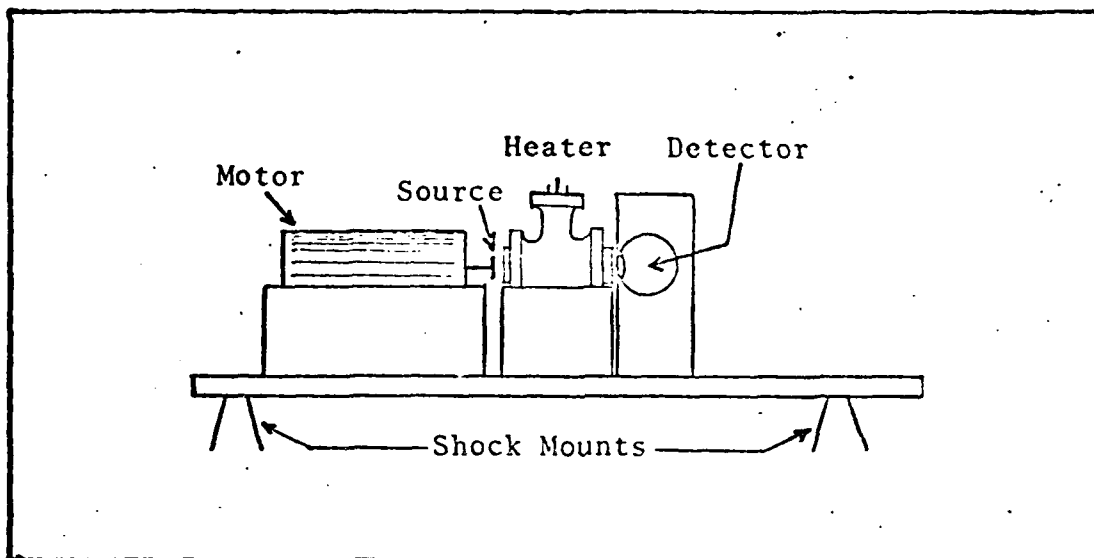
Fig 2. Mossbauer/Annealing System

a Lambda regulated DC power supply, was designed to provide
manually-set constant current. Because of the failure of this
power source, it was replaced with a Gardsman temperature
controller, which was connected through a filament transformer
to the heater. It supplied AC power, which produced an alter-
nating field between the heating elements. This produced a
problem which is discussed in Chapter IV. The edge thermo-
couple supplied feedback to the controller. Neither controller
regulated the temperature adequately; temperatures varied ±2 K
throughout the runs, with occasional drops (less than 1% of
annealing time) of up to 10 K.

A sketch of the source-absorber-detector   is
shown in Fig 2. The distance from the source to   ector
window was approximately 10 cm.

12

Sample Preparation

Dr. Harold Gegel, of the Air Force Materials Laboratory, provided the glassy metal ribbons which were used to prepare the samples. Battelle Laboratories at Columbus, Ohio, manufactured the ribbons by spin-cooling the molten alloy on a cooled rotating drum. The $Fe_{80}B_{20}$ (nominal atom percent) glass ribbons were 28.8 ± 0.5 µm thick, the $Fe_{80}P_{6.5}C_{3.5}B_{10}$ ribbons were 27.9 ± 0.5 µm thick, and the width of both varied from 0.5 to 1.2 mm with an average width of about 0.8 mm. The samples were prepared as a parallel array of the ribbons in 32 ± 2 mm long strips, to form an absorber 25 mm wide. The strips were held parallel with cellophane tape at the top and bottom and then bonded at one end with cyanoacrylate cement to a boron nitride disc (25.4 mm diameter). This was done to prevent thermal stresses which have been observed to affect the spectra (Ref 20). When the cement had dried, the glass strips were trimmed to the dimension of the boron nitride disc. Since the cement degraded during the annealing, the strips were held unfettered and remained free of thermal stress.

Heater Assembly

The sample and heating discs were assembled into the heater as shown in Fig 3. One graphite disc was inserted into the ceramic frame, followed by a clean boron nitride disc. The fine thermocouple was then centered on the boron nitride disc. The second boron nitride disc, with the glass sample attached, was then inserted, followed by the second graphite disc. The assembly was secured by two small plates and screws.
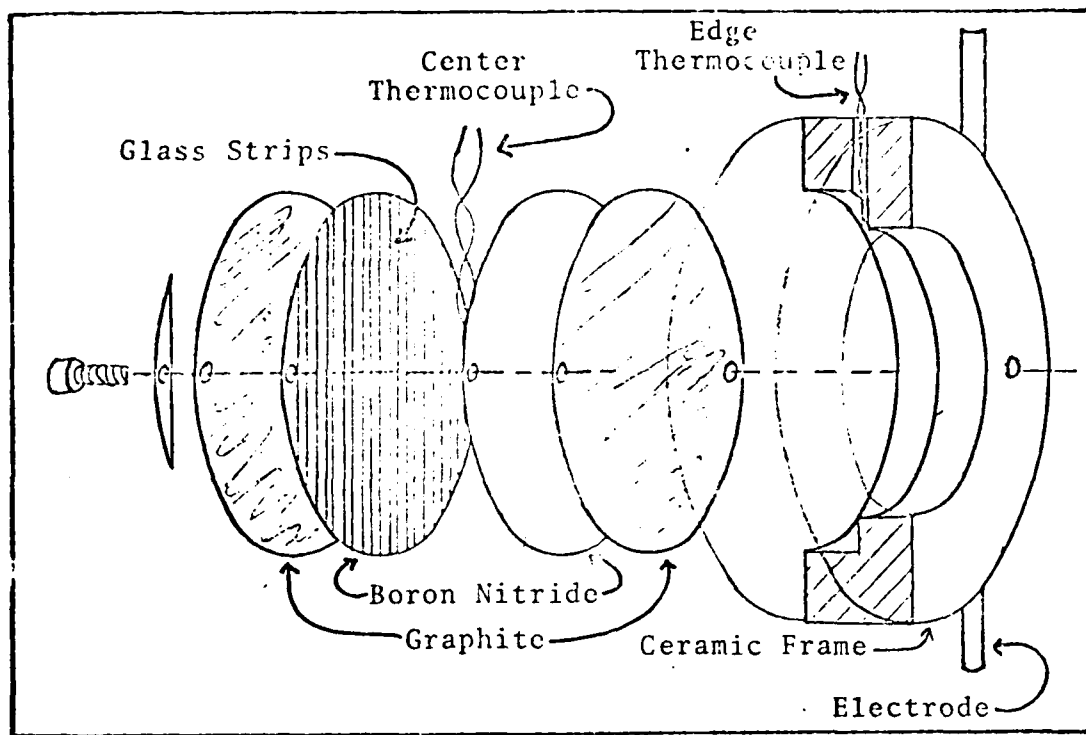
13

Fig 3.   Sample/Heater Assembly

The heater assembly was then inserted into the heater body, secured, and vacuum was applied.

Annealing and Data Collection

Once the heater was assembled and degassed overnight, the isothermal annealing run began.   The heating rate was 5 to 15 K/min up to 473 K, and held there until again degassed. When the vacuum dropped below 10^{-3} Pa, the temperature was increased to the desired annealing point.   Generally, this took about five minutes.   The initial Mossbauer spectrum was started as soon as this temperature was reached.   Additional spectra were then taken in sequence until the sample was near full

14

crystallization. The time between the end of one spectrum
and the beginning of the next was about ten minutes, which
was the time necessary to punch the 400 channels of data onto
paper tape. The isothermal annealing runs lasted from 10.5
hrs for $Fe_{80}B_{20}$ at 626 K, up to 315 hrs for $Fe_{80}B_{20}$ at 573 K.
To fully crystallize the samples, the temperature was in-
creased for about 18 hrs following each annealing run (to
640 K for $Fe_{80}B_{20}$, 750 K for $Fe_{80}P_{6.5}C_{3.5}B_{10}$). The tempera-
ture was then lowered to the original annealing point, and
a final Mossbauer spectrum was taken. The spectrum collection
periods were between 1 and 24 hrs, depending upon the crystal-
lization rate of the sample.

Data Processing

The Mossbauer spectra were analyzed by a least-squares
minimization curve fitting program developed at the Argonne
National Laboratory. This program, GENFIT, has been modified
by Skluzacek (Ref 1: 21), Schmidt (Ref 1: 21-22), and Roberts
(Ref 2: 18). It is listed as Appendix A of Roberts' thesis
(Ref 2: 50-60), and will not be repeated here. A user-
supplied subroutine, CALFUN, provides the mathematical model
to be fitted, along with the desired variable parameters.
Three different CALFUNs were used for this study. They are
explained below.

Subroutine CALFUN (Gaussian fit to $Fe_{80}B_{20}$ glass).
This subroutine fits Gaussian line shapes to the Fe glass
spectra taken at the beginning of each annealing run. Although

th... ...thod can lead to erroneous values of the average
hyperfine field (Ref 10: 478), it did provide reasonable fits.
Its purpose was to provide the glass spectra to be included
in the CALFUN below. The variables which were included in
this subroutine were:

1. Baseline: the average counts in the background
   of the Mossbauer spectrum.

2. Magnetic field: one value of average hyperfine
   field, in kOe (100 kOe = 7.96 MA/m).

3. Isomer shift: one value of average isomer shift
   for the glass, in mm/sec.

4. Quadrupole split: one value of average quadrupole
   split for the glass, in mm/sec.

5. Total intensity: one value for total intensity
   (average) of peaks one and six, expressed as a
   fraction.

6. Relative intensity: one value of the ratio of the
   average intensity of peaks two and five to the
   average intensity of peaks one and six.

7. Linewidths: six values of the full width at half
   maximum intensity (FWHM); one for each of the six
   Gaussian line shapes, in mm/sec.

The areal ratios of peaks three and four were constrained to
one-third the area of peak one. This subroutine is listed as
Appendix A. It was called GAUSSCALF.

   Subroutine CALFUN (Crystallized $Fe_{80}B_{20}$). This sub-
routine provides for fitting the data with one six-peak α-Fe

spectrum, three six-peak Fe_3B spectra, and one six-peak
(Gaussian) glass spectrum. The variable parameters are:

1. Baseline: as in GAUSSCALF above.

2. Magnetic fields: one hyperfine field for α-Fe
    and one each for three Fe_3B sites, in kOe.

3. Isomer shifts: one each for α-Fe and the three
    Fe_3P sites, in mm/sec.

4. Linewidths: one value of FWHM for peaks one and
    six, one for peaks two and five, and one for peaks
    three and four, of all three Fe_3B sites, in mm/sec.

5. Total intensities: one value of total intensity
    for each of α-Fe, Fe_3B, and the glass.

To simplify--and reduce the time and cost of--processing, this
subroutine required many constraints. The glass spectrum was
constrained to those parameters found in GAUSSCALF above, only
its intensity was variable. The linewidth of α-Fe was con-
strained to that value found for the fully crystallized spec-
trum, and all six peaks used this same value. The areal ratios
were 3:2:1:1:2:3 for peaks 1:2:3:4:5:6 of α-Fe and Fe_3B. The
relative intensities of the three Fe_3B sites were 1:1:1, and
their linewidths were constrained to be equal for similar peaks.
Finally, the quadrupole splits of α-Fe and the three Fe_3B sites
were constrained to zero. This subroutine, called INTFCALF,
is listed as Appendix B.

Subroutine CALFUN (for α-Fe, peaks one and six. This
version of CALFUN provides for analysis of only peaks one and
six of the α-Fe crystallized from the glass. It includes a

17

Gaussian shaped background, and does not fit the center por-
tion of the spectrum. The required variables are:

1. Baseline: as in GAUSSCALF.

2. Magnetic fields: one value for the α-Fe hyperfine
    field, and one value for the background, in kOe.

3. Total intensities: one value for the total inten-
    sity of peaks one and six of α-Fe, and one value
    for the background.

4. Linewidths: one value of FWHM for α-Fe, and one
    value for the background, in mm/sec.

5. Isomer shifts: one value of isomer shift for α-Fe
    and one value for the background, in mm/sec.

This subroutine is listed in Appendix C, and was called
ALPHA-BG. Appendix D contains instructions for using GENFIT
and CALFUN, and discusses required alterations to FIVECALF for
spectra taken at other temperatures.

Goodness of Fit

The goodness of fit to the Mossbauer spectra is measured
by Chi-squared, which is generated by GENFIT. Its value is
defined by:

$$Chi^2 = \sum_{i=1}^{N} \frac{(\text{data point}_i - \text{calculated point}_i)^2}{\text{data point}_i} \quad (5)$$

where N is the number of data points fitted. Theoretically,
the values of Chi-squared obtained for a number of spectra
should be randomly distributed around the number of data
points, in the limit approaching this number.

IV. Results and Discussion

In this section, the results of the spectra analyses
and crystallization rate determinations are presented. These
results are compared in the discussion to those derived by
others. Table I lists the isothermal annealing runs with
the sample material, temperature, annealing period, slope
of the Johnson-Mehl-Avrami plot, crystallization half-life
$t_{.5}$, and heater power (AC or DC). Figures 4 through 15 are
examples of the Mossbauer spectra taken during the annealing
runs. The title of each figure lists the sample material,
temperature, annealed time, CALFUN used, and crystalline
fraction. The crystalline fraction was calculated as the
ratio of the value of the α-Fe intensity of that run to the
value of the fully crystallized state. Figures 4 (2.89 hr
at 573 K) and 5 (48.9 hr at 573 K) show that the glass spec-
trum changes very little before crystallization. Figure 6
shows the α-Fe peaks just after the onset of crystallization;
note that the remainder of the spectrum still resembles the
glass spectra. Figures 7 an. , (19 and 100 percent crystal-
lized) include the locations of the peaks of the α-Fe and
three Fe_3B spectra, along with the values of their hyperfine
fields (in MA/m). Note that the values of the three Fe_3B
fields increased with time, which was true of all isothermal
annealing runs. However, the linewidths of these peaks de-
creased with time, as much as 50 percent. Figures 9 and 10

19

TABLE I

Annealing Runs

Run	Glass	Temperature (K ± 2 K)	Annealing Period (hr)	Half-life (hr)	Slope n	Power Type
1	$Fe_{80}B_{20}$	573	315	604 ± 57	1.60±0.22	DC
2	$Fe_{80}B_{20}$	604	45	34.0±.5	1.77±.24	AC
3	$Fe_{80}B_{20}$	611	76	18.0±0.7	1.50±0.06	DC
4	$Fe_{80}B_{20}$	611*	48	21.1±1.8	1.17±0.08	DC
5	$Fe_{80}B_{20}$	626	10.5	6.69±0.54	1.57±0.14	DC
6	$Fe_{80}P_{6.5}C_{3.5}B_{10}$	614	27	No crystallization observed		AC
7	$Fe_{80}P_{6.5}C_{3.5}B_{10}$	716	48	<2.9		AC
8	$Fe_{80}P_{6.5}C_{3.5}B_{10}$	744	25	<0.5		AC

*This sample was annealed 13 days at 573 K, and was about 22% crystallized at the beginning of this run.
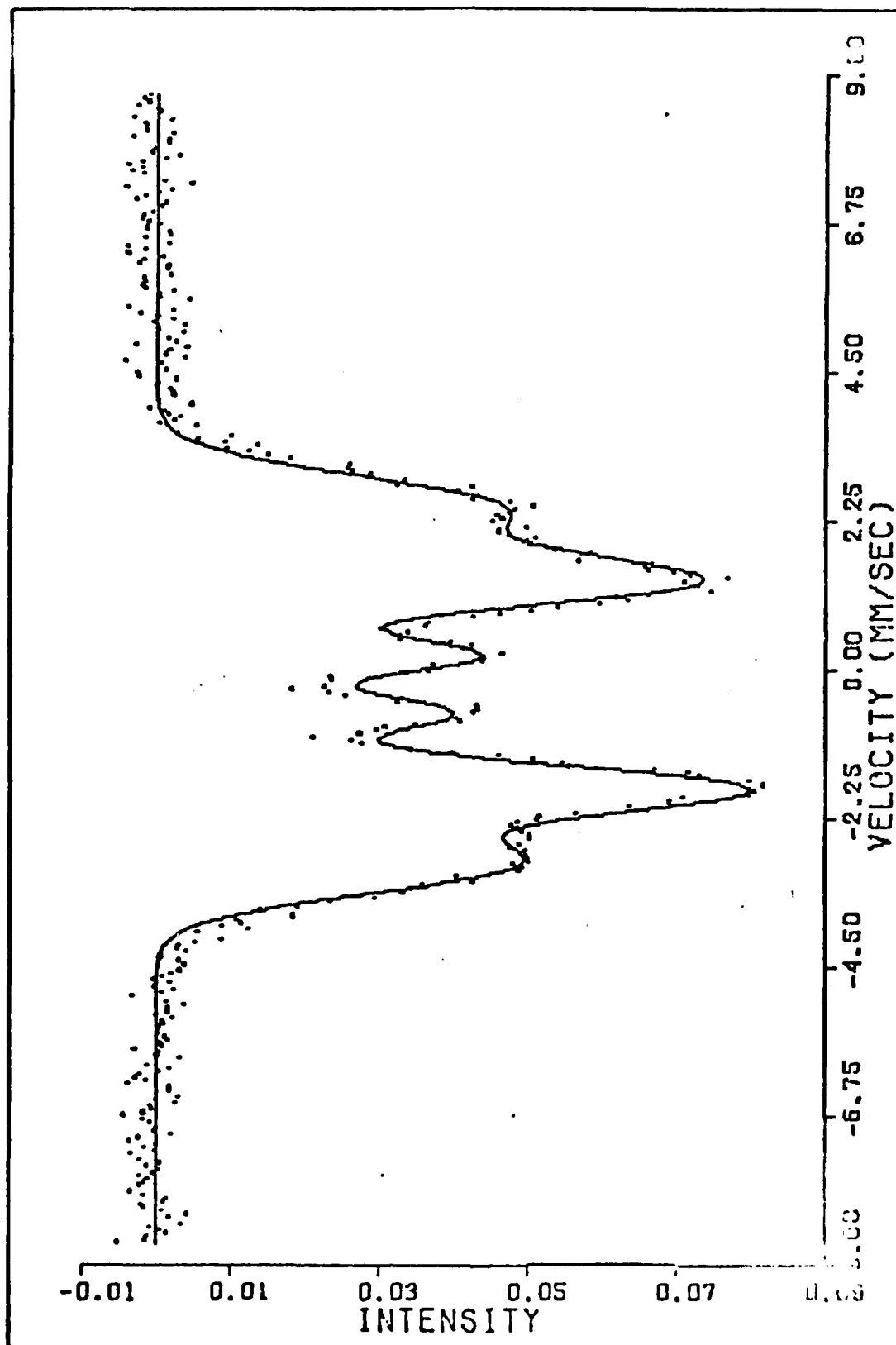
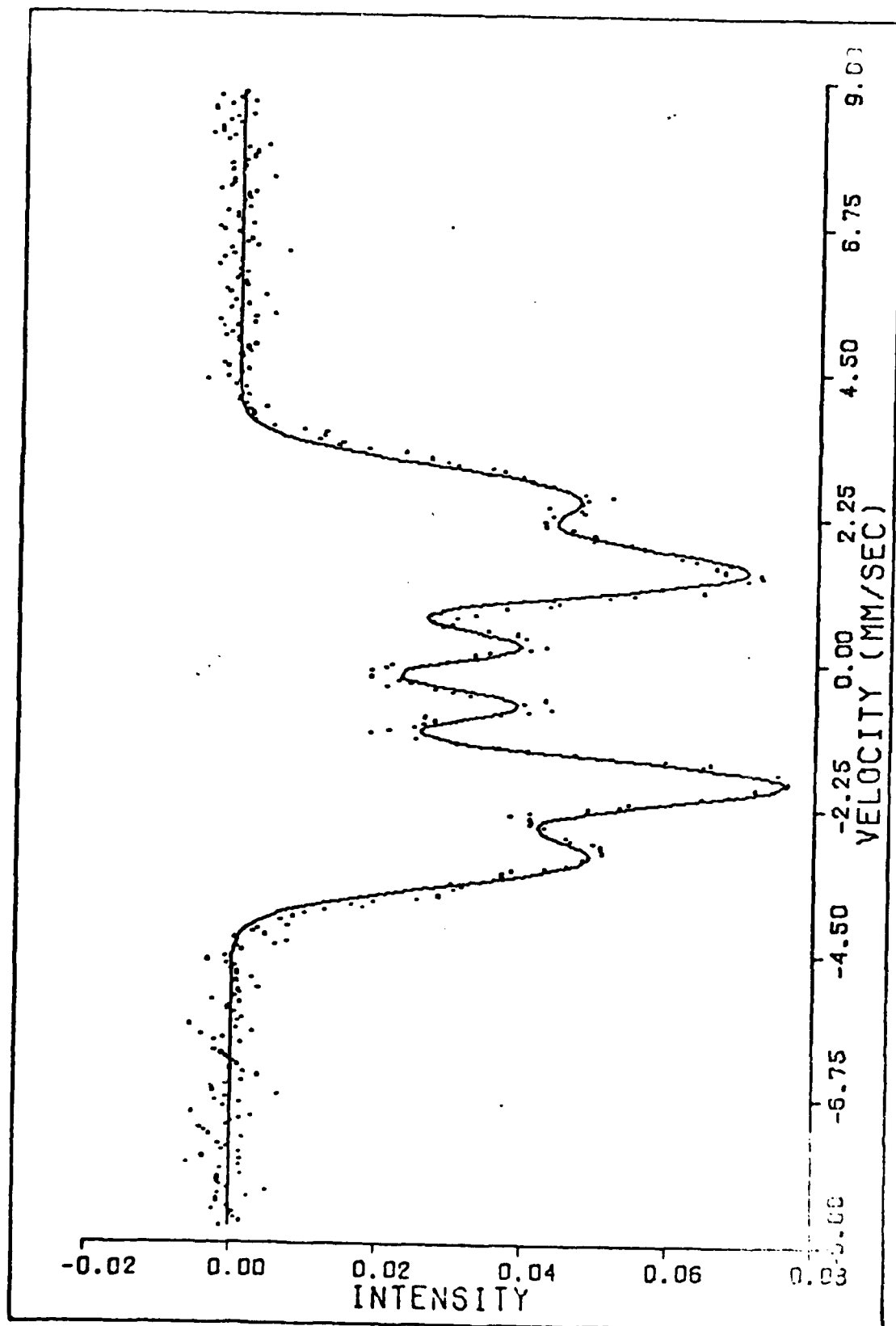Fig. 4. Mossbauer Spectrum of $Fe_{80}B_{20}$, 573 K, 2.08 Hr, GAUSSCALF, $x = 0$

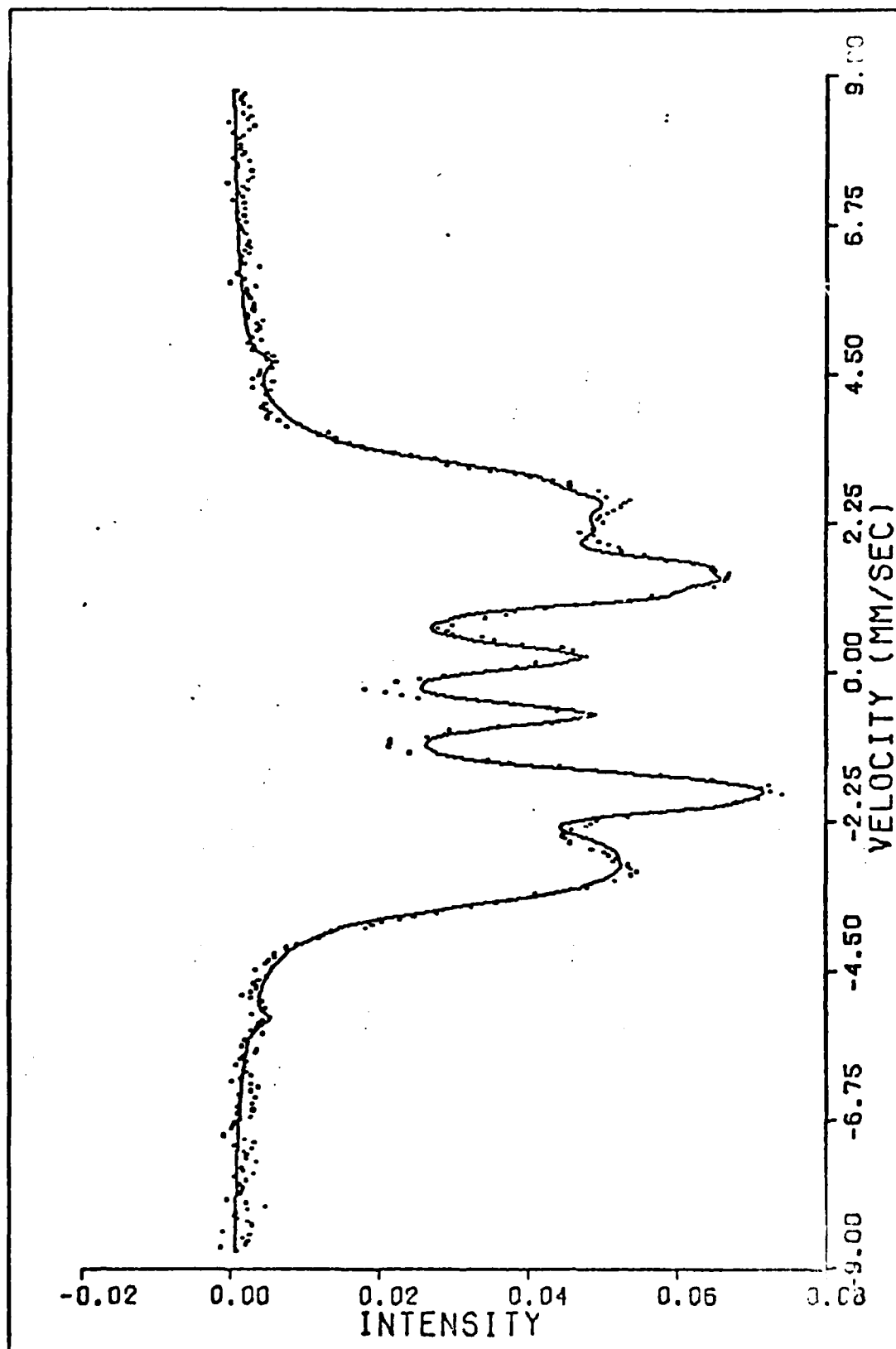Fig. 5. Mossbauer Spectrum of $Fe_{80}B_{20}$, 573 K, 48.9 Hr, GAUSSCALF, $x = 0$

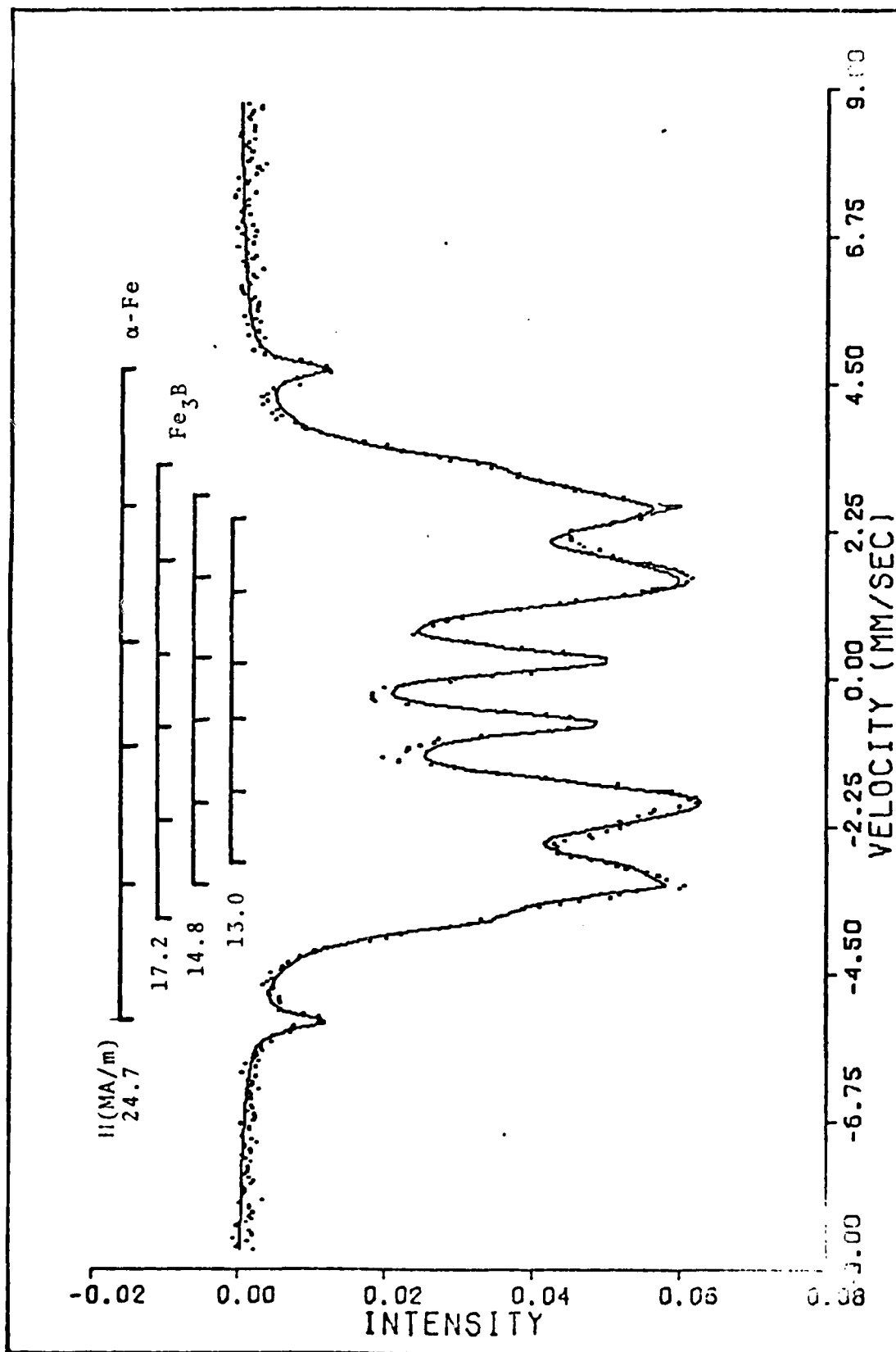Fig. 6. Mossbauer Spectrum of $Fe_{80}B_{20}$, 573 K, 111 IIr, FIVECALF, x = 0.0512

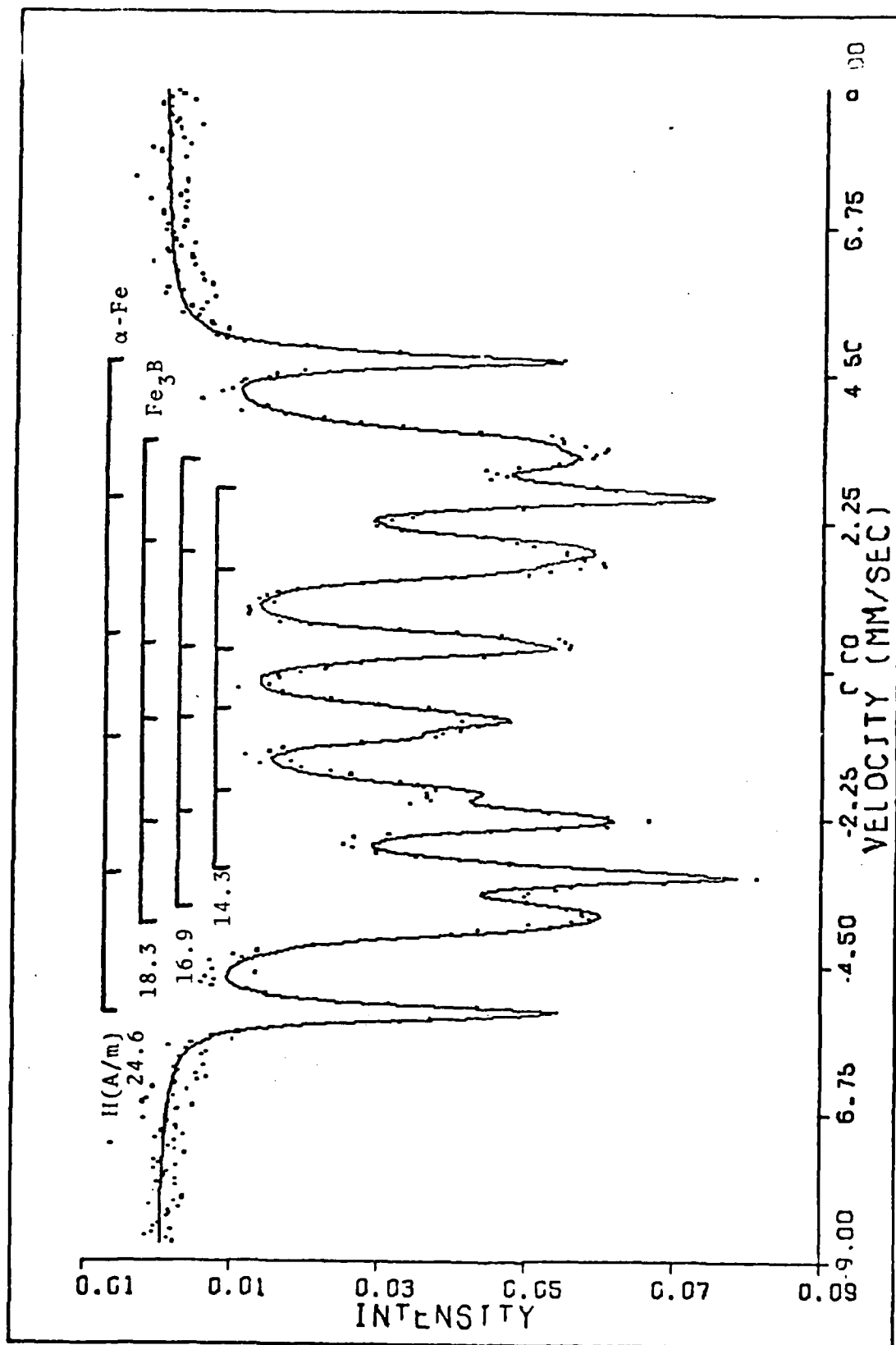Fig. 7. Mossbauer Spectrum of $Fe_{80}B_{20}$, 573 K, 281 Hr, FIVECALF, $x = 0.190$

Fig. 8. Mossbauer Spectrum of $Fe_{80}B_{20}$, 573 K, Fully Crystallized, FIVECALF

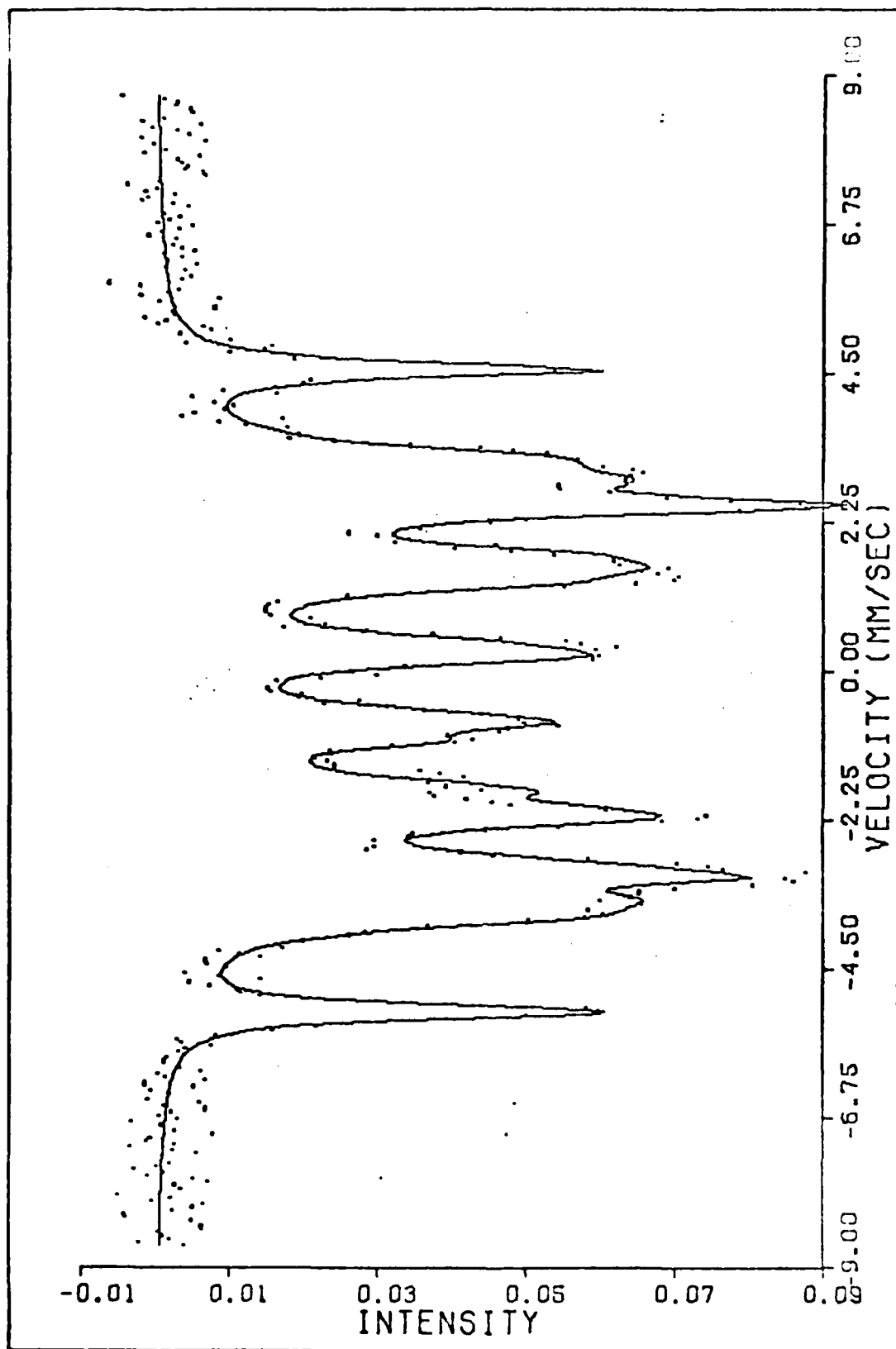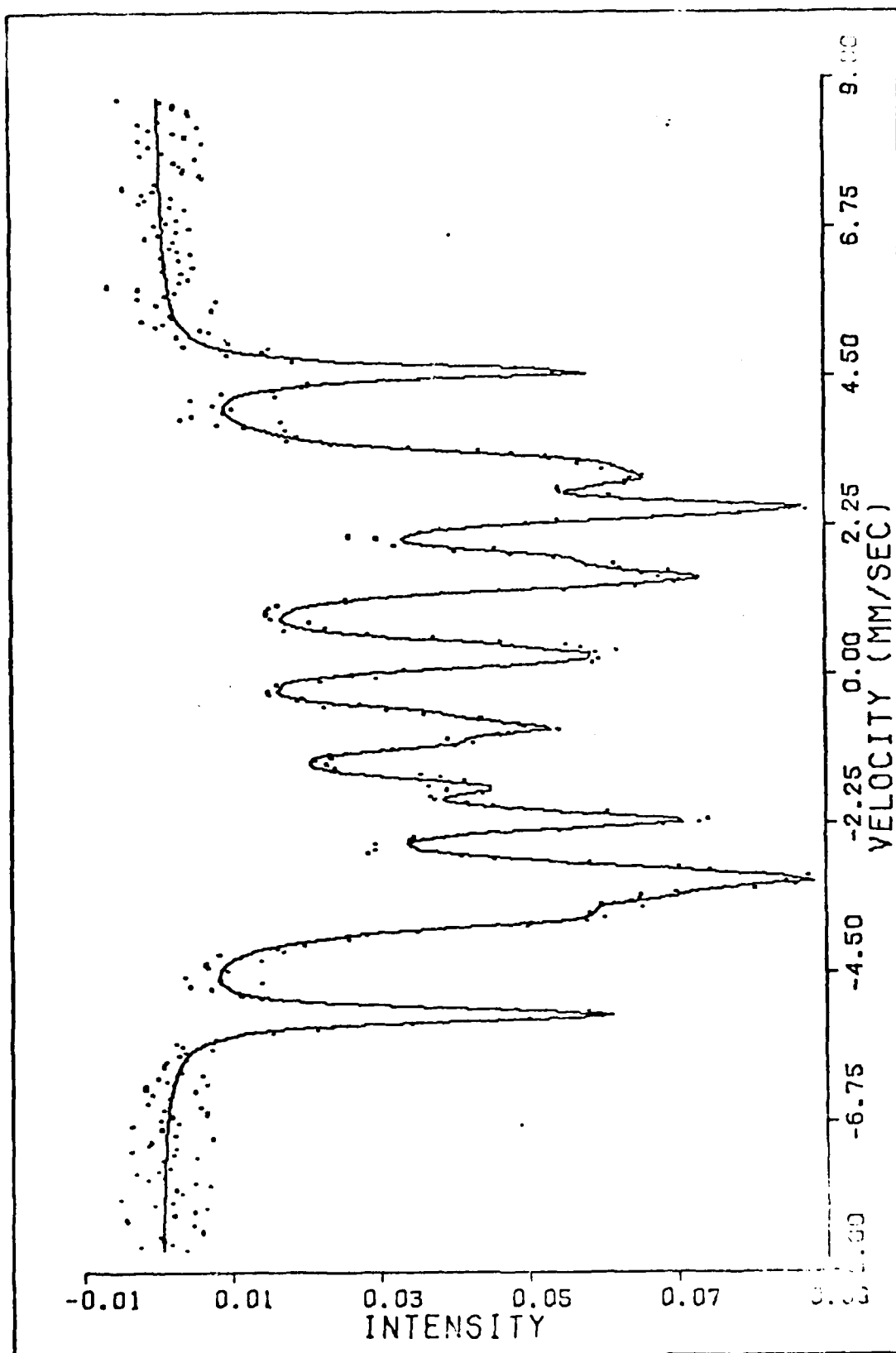Fig. 9. Mossbauer Spectrum of $Fe_{80}B_{20}$, 611 K, Fully Crystallized, FIVECALF

Fig 10. Mossbauer Spectrum of $Fe_{30}B_{20}$, 611 K, Fully Crystallized FIVECALF with Quadrupole Splitting

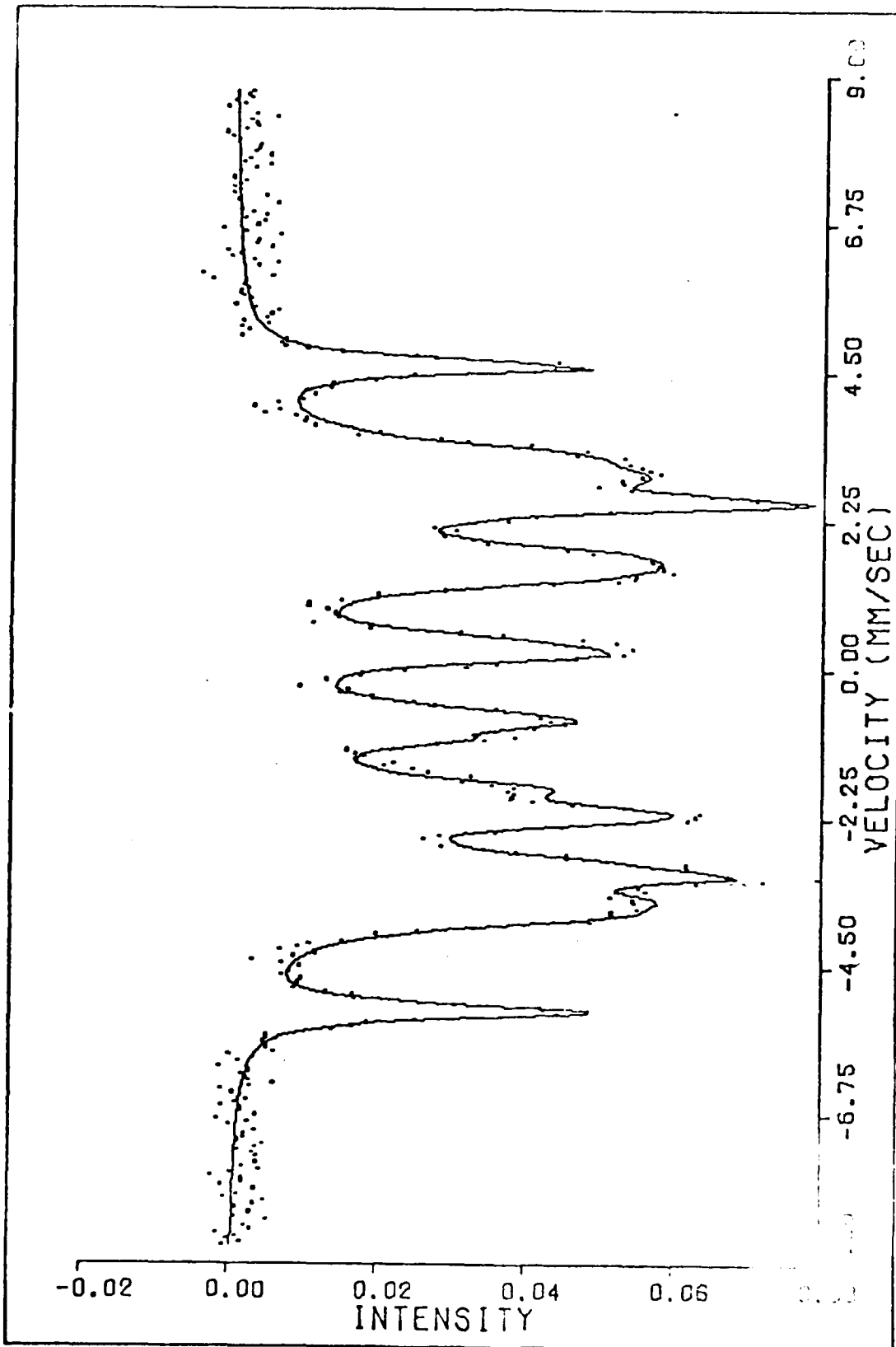Fig. 11. Mossbauer Spectrum of $Fe_{80}B_{20}$, 611 K, Run 3, Fully Crystallized
FIVECALF

28
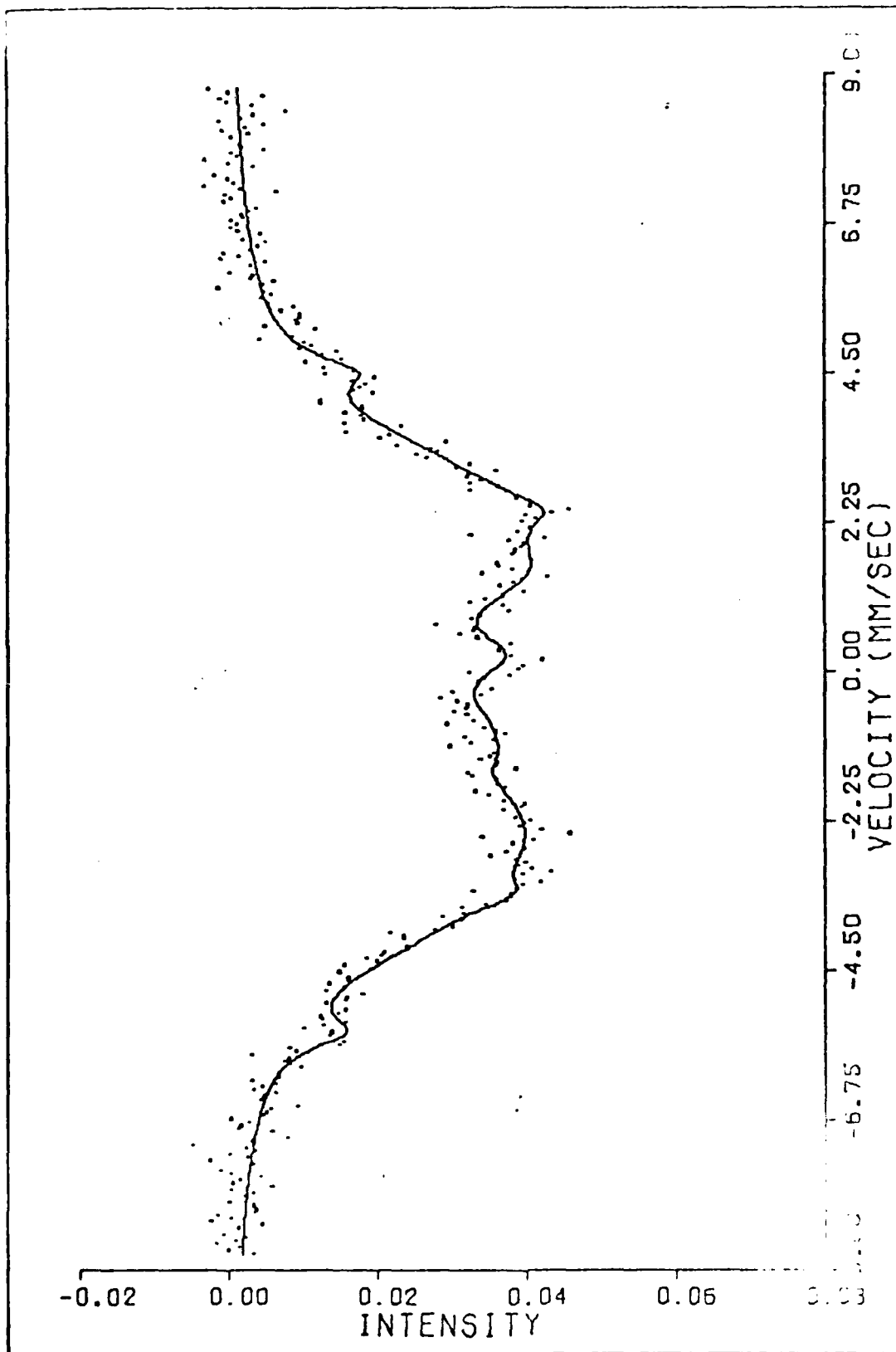
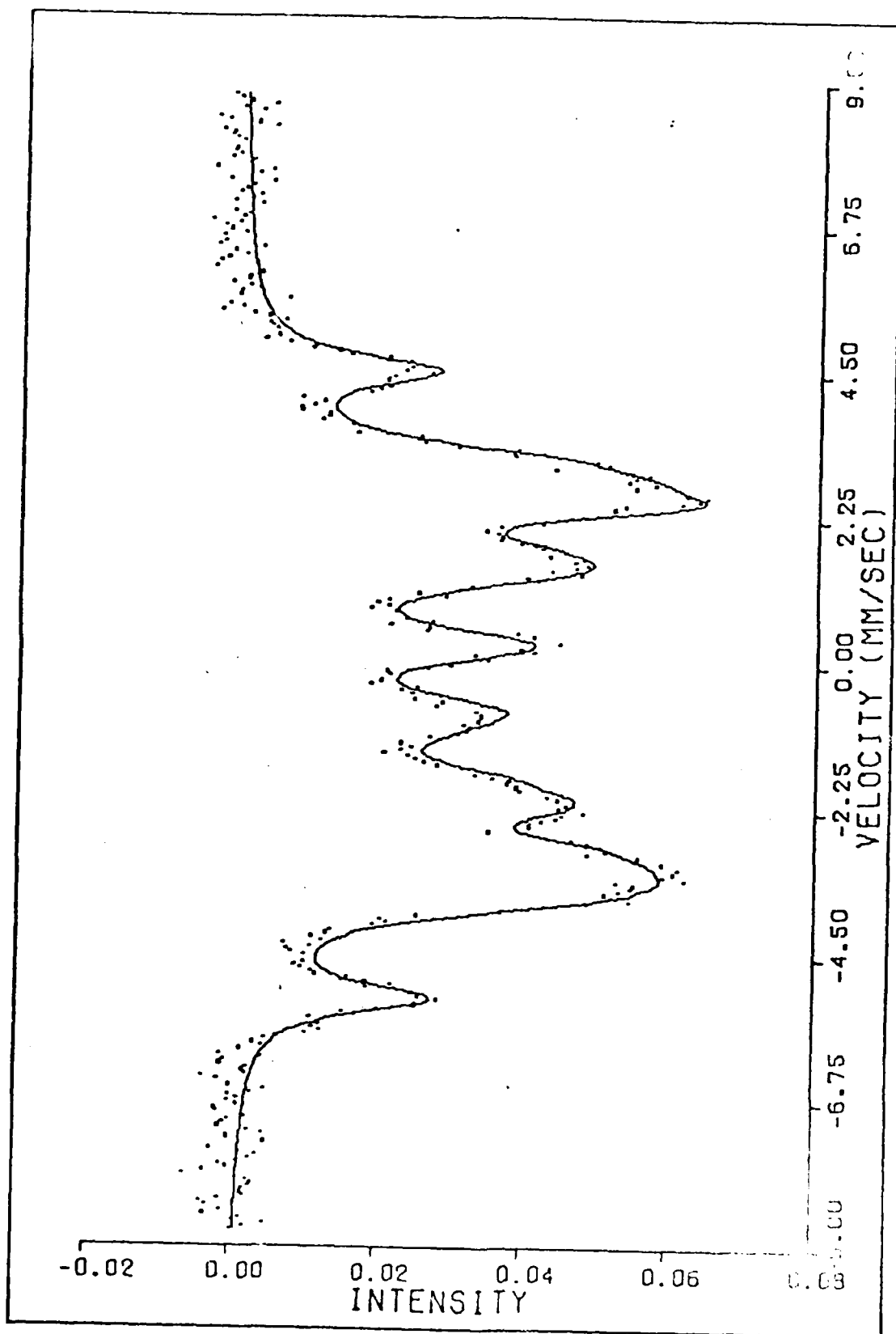Fig. 12. Mossbauer Spectrum of $Fe_{80}B_{20}$, 604 K, 13.8 Hr, FIVECALF, $x = 0.316$

Fig. 13. Mössbauer Spectrum of $Fe_{80}B_{20}$, 604 K, Fully Crystallized, FIVECALF

30

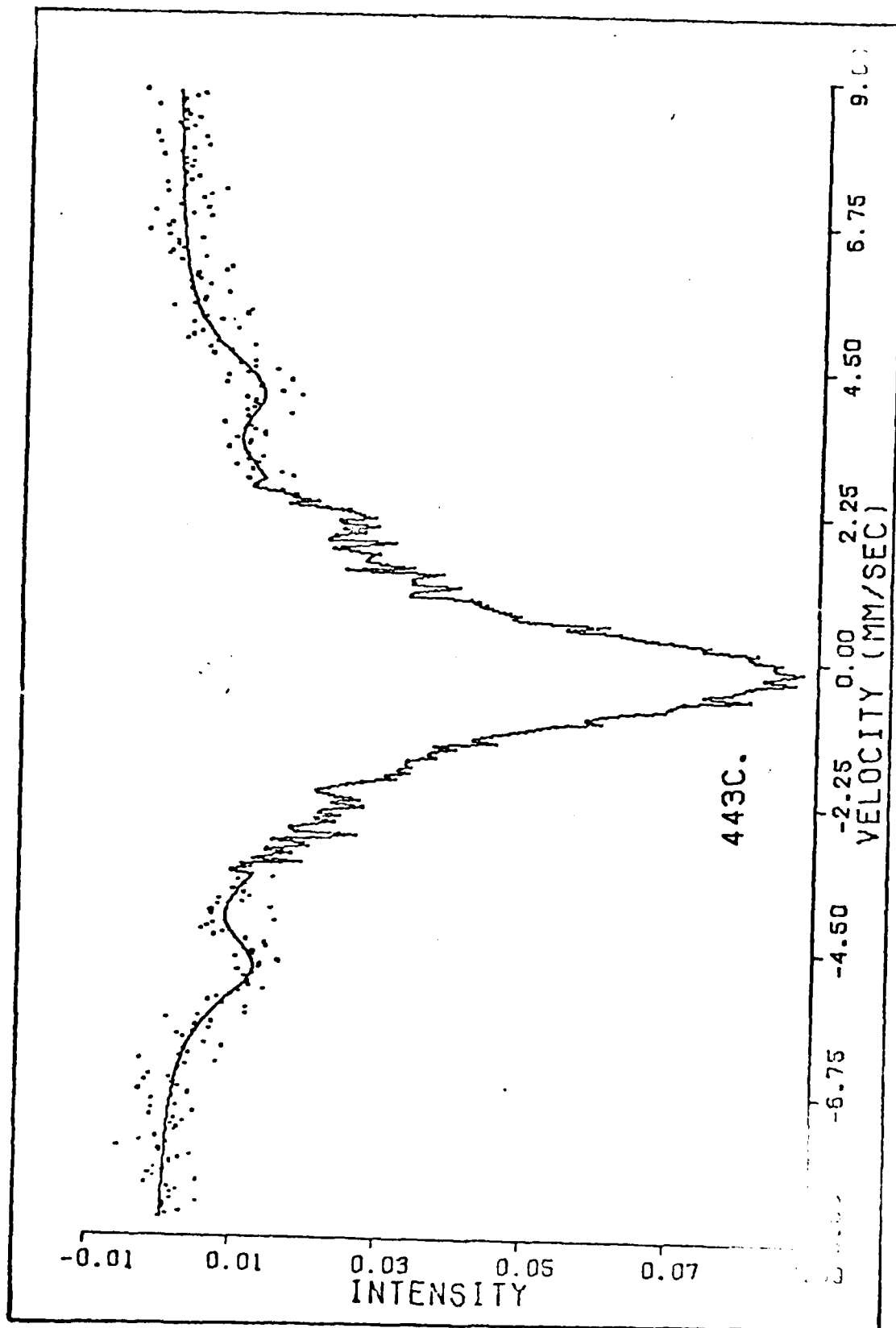Fig. 11. Mossbauer Spectrum of $Fe_{80}P_{6.5}C_{3.5}B_{10}$, 716 K, 2.87 Hr, ALPHA-BG, $x \cong 1$
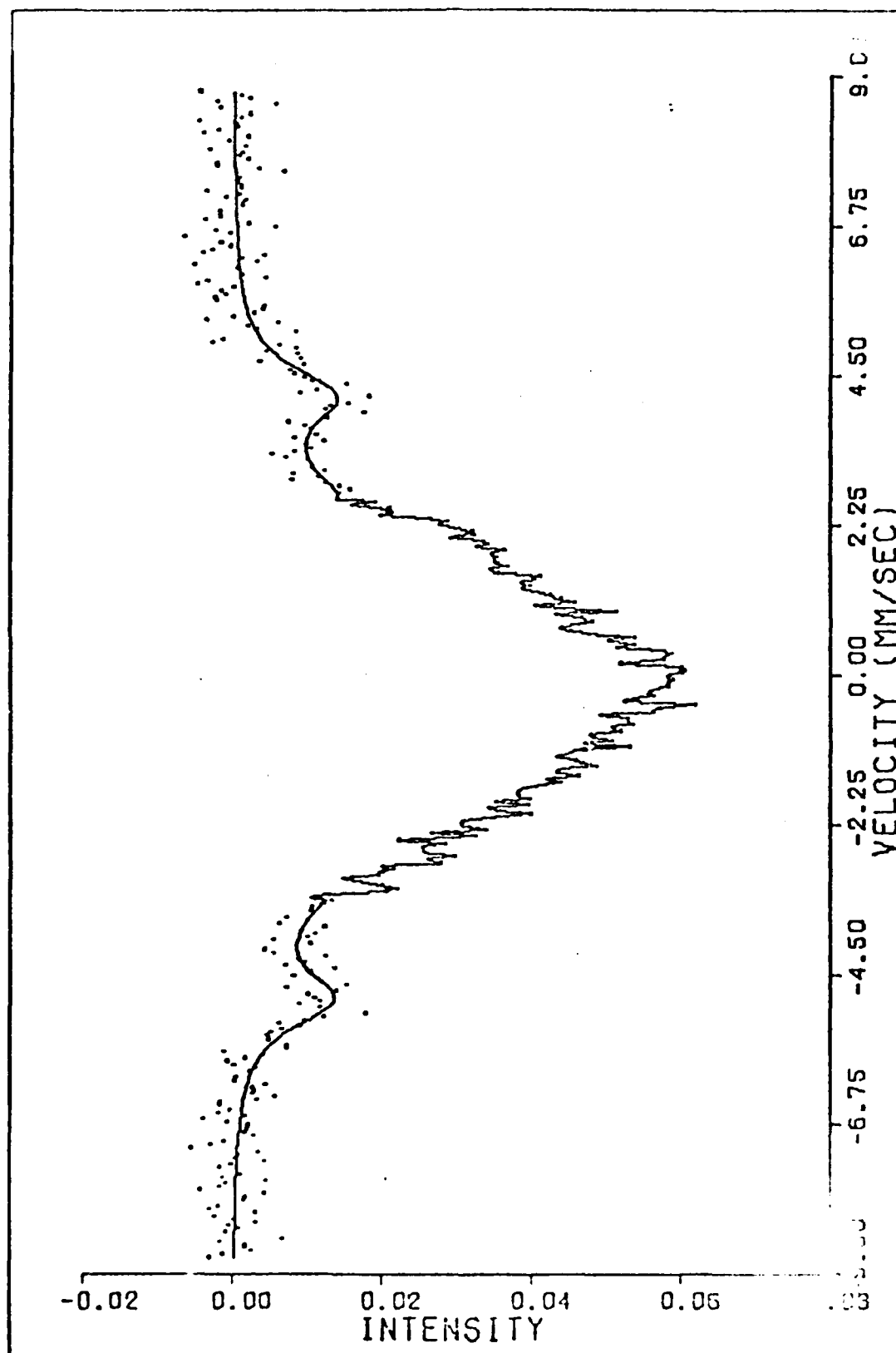
Fig. 15. Mossbauer Spectrum of $Fe_{80}P_{6.5}C_{3.5}B_{10}$, 716 K, Fully Crystallized
ALPHA-BG

clearly demonstrate the effect of constraining the both quadrupole splits to zero: Chi-squared was 508 for Fig 9, but with quadrupole splitting included in FIVECALF, it was 326 (for 330 data points). Figure 11 is the fully crystallized spectrum of Run 4, and except for total intensity, it is nearly identical to Fig 9 (Run 3 at the same temperature). Figures 12 and 13 show the poorly resolved spectra obtained when using AC power for the heater. Sample motion induced by an alternating magnetic field caused extreme line-broadening which resulted in overlapping of the absorption lines. Figures 14 and 15 are two spectra obtained with $Fe_{80}P_{6.5}C_{3.5}B_{10}$ (Run 7). Although the intensity of the α-Fe peak of Fig 14 indicated a fully crystallized state, visual inspection of these two spectra show a substantial change.

The crystallized fractions for $Fe_{80}B_{20}$ (Runs 1 thru 5) are plotted against time in Fig 16. Representative error bars are indicated on the first and last points of the 626 K data. The data of Run 4 were plotted such that the first data point fell on the calculated Run 3 line. Had the third data point been plotted on this line, the remaining points would have fallen very close to the Run 3 data. Because of low counts and line-broadening of the Mossbauer spectra of Run 2, only the last three data points were useable, and are included in Fig 16. The crystallization half lives, determine $\quad$ least-squares fits to the data of Fig 16 (between $x = 0.$ and $x = 0.80$). are plotted versus time in Fig 17. The value of the activation energy E_A for α-Fe crystallization was determined

33
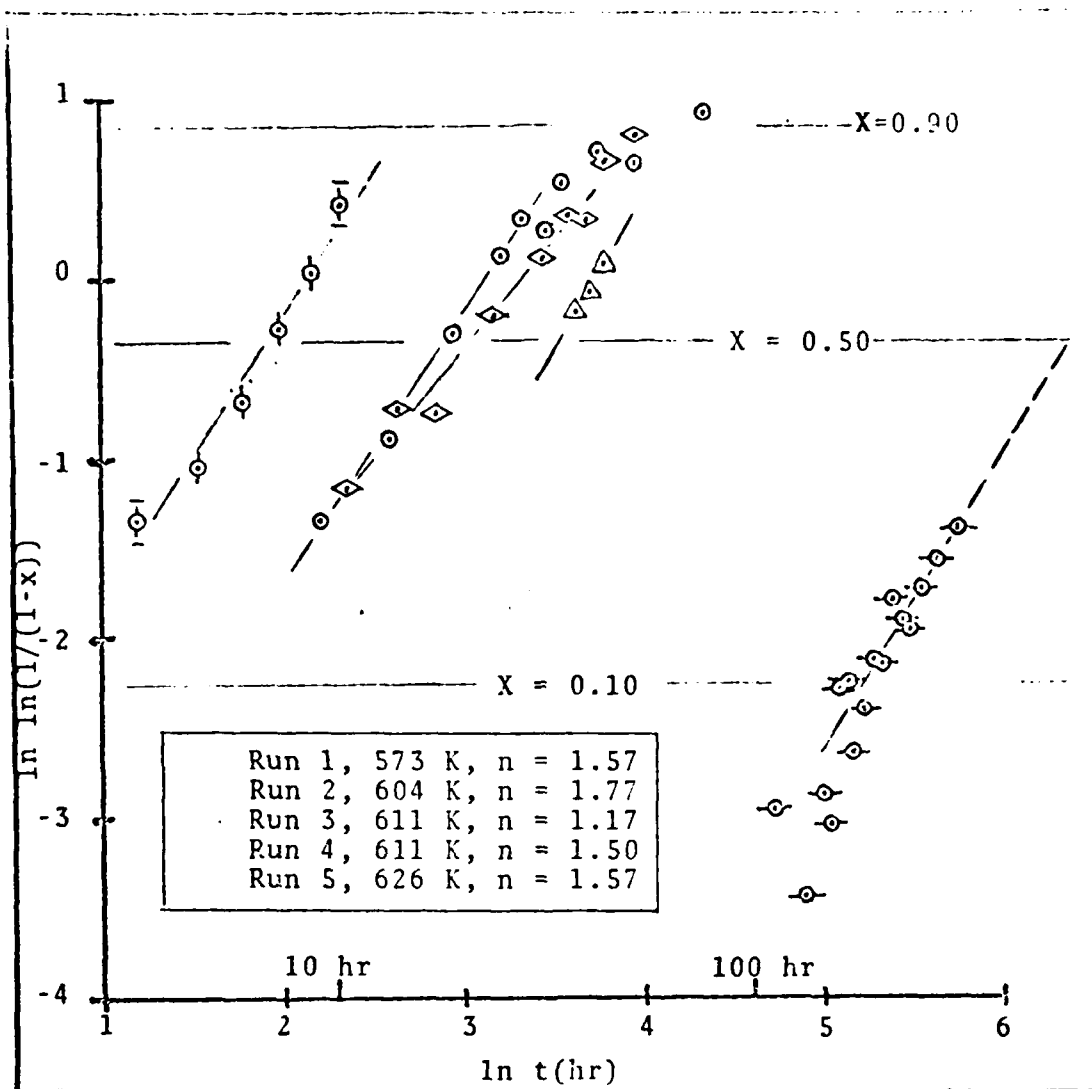
Fig 16. Crystallized Fraction x(t) vs Time,
Plotted as ln ln(1/(1-x)) vs ln t

The figure shows a plot with y-axis labeled $\ln \ln(1/(1-x))$ ranging from -4 to 1, and x-axis labeled $\ln t(hr)$ ranging from 1 to 6. Horizontal reference lines mark X=0.90, X = 0.50, and X = 0.10. Time markers at 10 hr and 100 hr.

Legend box:

Run 1, 573 K, n = 1.57
Run 2, 604 K, n = 1.77
Run 3, 611 K, n = 1.17
Run 4, 611 K, n = 1.50
Run 5, 626 K, n = 1.57

34

Fig 17. Arrhenius Plot. Crystallization
half lives of $Fe_{80}B_{20}$ versus time,
plotted as ln $t_{.5}$ vs 1000/T
(with 1σ error bars)

35

from a least-squares fit to the data of this Arrhenius plot. The value of E_A was 0.256 ± 0.006 MJ/mole (2.65 ± 0.07 eV/atom), and $\ln k_o^{-1}$ was -47.5. Using these constants and $T 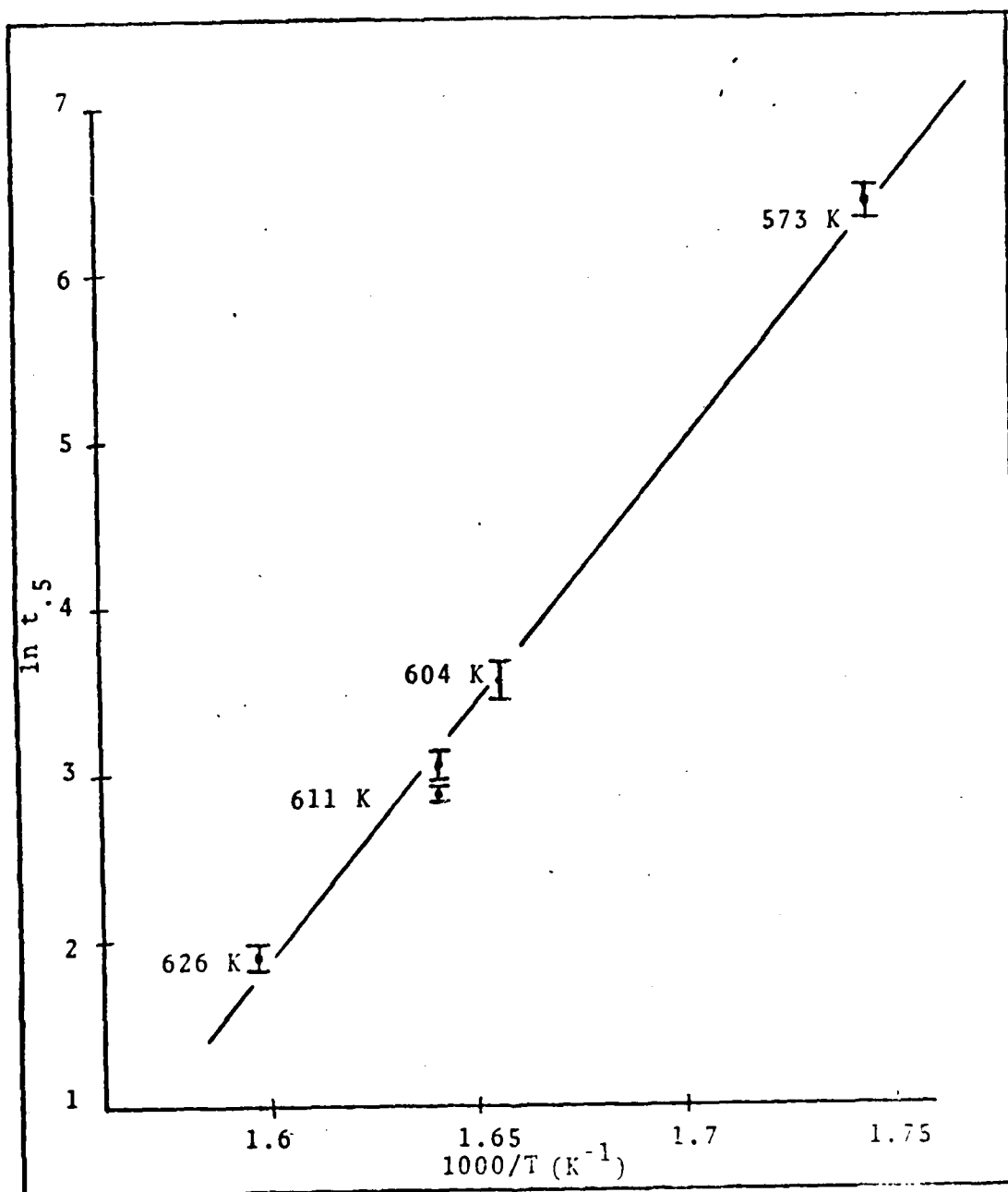= 473$ K in Eq (3), the predicted half-life of this $Fe_{80}B_{20}$ sample is 5500 ± 450 years at the expected operating temperature of 473 K.

The $Fe_{80}P_{6.5}C_{3.5}B_{10}$ did not crystallize at 614 K, but crystallized extremely fast at 716 and 744 K. Only one or two spectra were taken before full crystallization at these two temperatures. Hence, no kinetic data were obtained for this material. Only qualitative statements can be made about the crystallization of $Fe_{80}P_{6.5}C_{3.5}B_{10}$; these will be presented in the following section.

Discussion

The values of Chi-squared obtained when analyzing the Mossbauer spectra of Runs 1 through 5 varied over a large range--from less than the number of data points for some runs to up to four times the number of data points for others. This indicates a failure of the mathematical model used to describe the Mossbauer spectra. However, this failure was expected, considering the large number of constraints on the model used for FIVECALF (the values of Chi-squared for the GAUSSCALF and ALPHA-BG fits were generally very close to the number of data points). By visual inspection, the fits were good in the area of the α-Fe peaks, and its growth was probably followed accurately. The same cannot be said for the growth

of Fe_3B, due to the change in the hyperfine field and FWHM during crystallization. Since the glass spectrum does broaden slightly during crystallization, it may continue to change throughout the transformation. The fit to the Fe_3B spectra would then have to account for this change. An alternative view might be to consider the Fe_3B as still semi-amorphous during crystallization.

In Mossbauer spectra taken during early annealing runs, the values of FWHM for the Fe_3B peaks increased for peaks farther from the center. This is typical of glass spectra (Ref 16: 821). For the fully crystallized spectra, the FWHM's were nearly constant, which indicates a crystalline state. This view tends to support Kemeny's (Ref 10: 485) and Schaafsma''s (Ref 11: 4429) conclusions that crystal nuclei exist in the as-quenched glass and that the structure should be based on a locally distorted, quasi-crystalline Fe_3B. It appears that the material is transformed from a glass to a semi-amorphous Fe_3B, and finally to a tetragonal Fe_3B crystal. This may be due to a stress relaxation rather than a crystallization process.

Because of the long time required to reach full crystallization at 573 K, Run 1 was terminated at 315 hrs, and the temperature was raised to 611 K. This was done to try to detect a change in the crystallization process at the lower temperature. The first crystallization time of Run 4 was adjusted by Δt so that this data point fell on the line calculated for Run 3. The other times of Run 4 were then adjusted by this

37

s   , and the data was compared to that of Run 3. Because
o: the data scatter, no conclusion was made concerning a change
in the crystallization rate or process.

Using the methods described in Chapter I, others have
found the activation energy of $Fe_{80}B_{20}$ to be between 0.195 and
0.257 MJ/mole, with the average toward the upper value (Refs 3:
42; 6: 139; 10: 485; 11: 4427). This range is significant:
Luborsky, using calorimetric and magnetic methods to measure
the onset of crystallization in $Fe_{80}B_{20}$, determined that the
activation energy was 0.202 MJ/mole. He used this value to
calculate an expected lifetime of 25 years at 473 K. He deter-
mined that "after the onset of crystallization, the magnetic
properties deteriorate catastrophically [Ref 3: 139]."
Schaafsma determined that the onset of crystallization corres-
ponds to a crystallized fraction of less than 0.02 (Ref 11:
4425). Using his data, with E_A = 0.242 MJ/mole, to calculate
the onset of crystallization, the projected lifetime of his
glass is 1000 years at 473 K. The same calculation yields a
lifetime of 400 years at 473 K for the $Fe_{80}B_{20}$ of this study.
These calculations assume that the crystallization rate is
determined by the growth of α-Fe, not Fe_3B; and that the crys-
tallization mechanism does not change between 573 and 473 K.

The data obtained during the crystallization of
$Fe_{80}P_{6.5}C_{3.5}B_{10}$ were insufficient for analysis of its crystal-
lization kinetics. However, a much higher temperature was
required for crystallization. Therefore, qualitatively, its
activation energy would be greater than that of $Fe_{80}B_{20}$. This

is true for other similar glasses with many atomic species
(i.e., $Fe_{40}Ni_{40}B_{20}$, $Fe_{80}P_{13}C_7$, $Fe_{40}Ni_{40}P_{14}B_6$, Ref 3: 140).
Thus, the lifetime of $Fe_{80}P_{6.5}C_{3.5}B_{10}$ is expected to be greater
than that of $Fe_{80}B_{20}$.

V. Conclusions and Recommendations

The metallic glasses $Fe_{80}B_{20}$ and $Fe_{80}P_{6.5}C_{3.5}B_{10}$ have been crystallized by isothermal annealing at high temperatures. The crystallization was followed with Mossbauer spectroscopy, and the rates of formation of α-Fe crystals in $Fe_{80}B_{20}$ were determined. These rates were used to determine the activation energy and rate constant of the crystallization process. These constants were used to calculate the expected lifetime of $Fe_{80}B_{20}$ at 473 K, 100 K below the lowest isothermal run. If the crystallization mechanism does not change between 473 and 573 K, the onset of crystallization is projected to be approximately 400 years. No kinetic data were obtained for the crystallization of $Fe_{80}P_{6.5}C_{3.5}B_{10}$, or for the formation of Fe_3B in the $Fe_{80}B_{20}$.

Recommendations

This study can be expanded in the following ways:

1) Use a stronger Mossbauer source to increase counts per channel. This would permit a more careful study of the crystallized spectra to determine Fe_3B growth rates.

2) Use an accurate temperature controller (with direct current), and continue the study at lower temperatures.

3) Study the magnetic and material properties of partially crystallized samples. This would relate crystallized fraction to material performance.

40

4) Since an alternating field can accelerate the aging of the glass (Ref 12), include a strong rf field during some of the isothermal annealing runs. The field strength must be great enough to displace the atoms in the amorphous metal. Kopcewicz found that 800 A/M at 67 MHz was enough to cause crystallization, but 400 A/M at 53 MHz was not.

Bibliography

1. Schmidt, T.A. "An Analysis of Metallic Glasses by Mossbauer Spectroscopy." Unpublished MS thesis. Wright-Patterson AFB, Ohio: School of Engineering, Air Force Institute of Technology March 1978.

2. Roberts, L.D. "Mossbauer Studies of Metallic Glasses." Unpublished MS thesis. Wright-Patterson AFB, Ohio: School of Engineering, Air Force Institute of Technology, December 1978. AD A064049.

3. Luborsky, F.E. "Crystallization of Some Fe-Ni Metallic Glasses," Materials Science and Engineering, 28: 139-144 (1977).

4. Fukamichi, K., et al. "Invar-type New Ferromagnetic Amorphous Fe-B Alloys," Solid State Communications, 23(12): 955-958 (September 1977).

5. Chien, C.L. "Mossbauer Study of a Binary Amorphous Ferromagnet: $Fe_{80}B_{20}$," Physical Review B, 18(3): 1003-1015 (1 August 1978).

6. Luborsky, F.E. and H.H. Lieberman. "Crystallization Kinetics of Fe-B Amorphous Alloys," Applied Physics Letters, 33(3): 233-234 (1 August 1978).

7. Tarnoczi, T., et al. "The Role of Fe_3B Compound in the Crystallization of Fe-B Metallic Glasses," IEEE Transactions on Magetism, Mag-14(5): 1025-1027 (September 1978).

8. Matsuura, M. "Crystallization Kinetics of Amorphous Fe-B Alloys by DTA," Solid State Communications, 30(4): 231-233 (April 1979).

9. Chien, C.L., et al. "Magnetic Properties of Fe_xB_{100-x} ($72 \leq x \leq 86$) and Crystalline Fe_3B," Physical Review B, 20(1): 283-295 (1 July 1979).

10. Kemeny, T., et al. "Structure and Crystallization of Fe-B$_x$ Metallic Glasses," Physical Review B, 20(2): 47-488 (15 July 1979).

11. Schaafsma, A.S., et al. "Amorphous to Crystalline Transformation of $Fe_{80}B_{20}$," Physical Review B, 29(11): 4423-4430 (1 December 1979).

12. Kopkewicz, M. "Radio-Frequency Annealing Effects in Amorphous $Fe_{40}Ni_{40}B_{20}$," Applied Physics, 23(1): 1-6 (September 1980).

13. May, L. An Introduction to Mossbauer Spectroscopy. New York: Plenum Press, 1971.

14. Gonser, Uli. "From a Strange Effect to Mossbauer Spectroscopy," in Topics in Applied Physics, Volume 5: Mossbauer Spectroscopy, edited by Uli Gonser. New York: Springer-Verlag, 1975.

15. Vincze, I. "Evaluation of Complex Mossbauer Spectra in Amorphous and Crystalline Ferromagnets," Solid State Communications, 25(9): 689-693 (March 1978).

16. Schurer, P.J. and A.H. Morrish. "Continuous Versus Discrete Hyperfine-Field Distributions in Amorphous Ferromagnetic Iron Alloys," Solid State Communications, 28(9): 819-823 (December 1978).

17. Hesse, J. and A. Rubartsh. "Model Independent Evaluation of Overlapped Mossbauer Spectra," Journal of Physics E, 7(6): 526-532 (June 1974).

18. Schurer, P.J. and A.H. Morrish. "Mossbauer Study of Magnetic Anisotropy in Amorphous $Fe_{40}Ni_{38}Mo_4B_{18}$," Journal of Magnetism and Magnetics, 15-18: 577-578 (1980).

19. Skluzacek, E.W. "Analysis of the Mossbauer Spectra of $NdCo_5$." AFML-TR-75-162. Wright-Patterson AFB, Ohio: Air Force Materials Laboratory, 1976.

20. Lafleur, L.D. "Mossbauer Study of Stress-Induced Rotation of Magnetization in Amorphous $Fe_{80}B_{20}$," Physical Review B, 20(7): 2581-2585 (1 October 1979).

GAUSSCALF

```
      SUBROUTINE CALFUN(NP,NPAR,F,X)

C     THIS VERSION OF CALFUN USES A GAUSSIAN LINE SHAPE TO FIT THE
C     ABSORPTION SPECTRUM OF A METALLIC GLASS.  IT GIVES ONE AVERAGE
C     VALUE FOR HYPERFINE FIELD, ONE FOR ISOMER SHIFT, AND ONE FOR
C     QUADRUPOLE SPLIT.  IT GIVES A LINEWIDTH FOR EACH OF THE SIX
C     PEAKS, AND THE INTENSITY RATIO OF PEAK 2 TO PEAK 1. THE AREAL
C     RATIO FOR PEAKS 3 AND 4 TO PEAK 1 IS 1:3. THESE VALUES CAN
C     THEN BE SUBSTITUTED INTO THE CALFUN CALLED FIVECALF, TO PERMIT
C     FITTING THE CRYSTALLIZED GLASS SPECTRA.
C
C             GAUSSCALF    15 OCT 80
C
C     THE REQUIRED VARIABLES ARE:
C
C         ONE VALUE FOR H-FIELD: X(1)
C
C         ONE VALUE OF ISOMER SHIFT: X(2)
C
C         ONE VALUE OF QUAD SPLIT: X(3)
C
C         ONE VALUE FOR TOTAL INTENSITY OF PEAK 1: X(4)
C
C         ONE VALUE FOR RELATIVE INTENSITY TO PEAK 1: X(5)
C
C         SIX VALUES OF LINE WIDTH: X(6), TO X(11)
C
C         BASELINE IS LAST VARIABLE: X(12)
C
C         TOTAL OF 12 VARIABLES REQUIRED
C
      COMMON W(13,01),XD(402),YD(402),YS(402),YDY(402),YCY(402),FSQ(402)
      COMMON /HEADING/TITL(18)
      COMMON /NAM/XINIT(25),PRM(25),ERX(25),NBASE
      COMMON /CALF/ IFLAG
      DIMENSION F(402),X(25)
      REAL V(6),MHEX,MUGND,MUSUBN,LIGHT
```

```
C
C     LOAD VALUES OF BINOMIAL PROBABILITIES
C
C
      MUEX=.15491
      MUGND=-.944206
      R=MUEX/(MUGND*2.)
C
C     FACTOR CONVERTS FROM ENERGY UNITS TO VELOCITY UNITS.
C
C                GZERO*MUSUBN*LIGHT*F1*F2
C     FACTOR =   ------------------------
C                     2.*EZERO*F3
C
C
      GZERO=.18948
      MUSUBN=5.04E-27
      LIGHT=2.998E11
      F1=1.0E-3
      F2=1.0E-4
      EZERO=14.4125E3
      F3=1.6.2E-15
C
      FACTOR=(GZEFO*MUSUBN*LIGHT*F1*F2)/(EZERO*F3*2.)
C
      A = FACTOR*(3.*R-1.)
      B = FACTOR*( R-1.)
      C = FACTOR*( R+1.)
C
      IF(IFLAG)25,25,10
C
C     IF FLAG IS NOT POSITIVE CALFUN IS BEING CALLED FOR PRINTING ONLY
C
   10 CONTINUE
C
C     CALCULATE PEAK VELOCITIES FOR EACH SITE
C
      C=X(2)
      D=X(3)/2.
```

```
      X(1)=ABS(X(1))
      Y(1)=A*X(1)+S+Q
      Y(2)=D*X(1)+S-Q
      Y(3)=-C*X(1)+S-Q
      Y(4)=C*X(1)+S-Q
      Y(5)=-D*X(1)+S-Q
      Y(6)=-A*X(1)+S+Q
      DO 33 I=,11
      Y(I)=ABS(X(I))
33    
25    CONTINUE
C
C     CALCULATE THE SPECTRUM
C
C
      RFL=X(6)*X(7)/X(6)
      IF(RFL.GT.1.4) X(5)=1.4*X(6)/X(7)
      DO 7? I=1,NP
      YC(I)=0.
      DO 35 K=1,6
      IF(K.EQ.1) TI=X(4)
      IF(K.EQ.2) TI=X(4)*X(5)
      IF(K.EQ.3) TI=X(4)*X(6)/(3.*X(8))
      IF(K.EQ.4) TI=X(4)*X(6)/(3.*X(3))
      IF(K.EQ.5) TI=X(4)*X(5)*X(7)/X(10)
      IF(K.EQ.6) TI=X(4)*X(6)/X(11)
      KP5=K+5
      YYY=(X0(I)-V(K))**2/(2.*X(KP5)*.4247*X(KP5)*.4247*X(KP5)*.4247)
      IF(YYY.GT.18.) YYY=18.
35    YC(I)=YC(I)+(TI/SQRT(6.2832*X(KP5)*.4247*X(KP5)*.4247))*EXP(-YYY)
      YC(I)=(1.-YC(I))*X(NBASE)
3L    F(I)=(YD(I)-YC(I))/SQRT(YD(I))
      RETURN
C
C     ON THE FINAL CALL OF CALFUN PRINT THE PEAK VELOCITIES
C
25    CONTINUE
      PRINT 9C
```

46

```
PRINT *,""                                    001240
PRINT *,""                                     001250
PRINT *,"   THE PEAK VELOCITIES   ARE:"         001260
PRINT *,""                                      001270
PRINT 100,(V(I),I=1,6)                          001280
PRINT *,""                                      001290
PRINT *,""                                      001300
91   FORMAT(1H1)                                001310
100  FORMAT(5X,7F10.4)                          001320
     RETURN                                     001330
     END                                        001340
```

47

FIVECALF

```
      SUBROUTINE CALFUN(NP,NPAR,F,X)

C
C   CALFUN USES SUPERPOSITION OF FIVE 5-PEAK SPECTRA: ONE FOR
C   ALPHA-FE, THREE FOR FE3B, AND ONE FOR THE GLASS.  THE VARIABLE
C   PARAMETERS ARE LISTED BELOW.  THE LINEWIDTH FOR ALPHA-FE MUST
C   BE ADDED AT LINE 1731.  AREA RATIOS ARE NORMALIZED TO PEAK 1
C   FOR EACH SPECTRUM.  ALL THREE FE3B SPECTRA ARE REQUIRED TO HAVE
C   THE SAME AMPLITUDE, AND AREA RATIOS FOR PEAKS 1:2:3:4:5:5 OF
C   3:2:1:1:2:3.  FOR THE GLASS SPECTRUM, ONLY THE INTENSITY IS A
C   VARIABLE PARAMETER, THE OTHERS MUST BE SUPPLIED IN LINES 1467
C   TO 1487 AND 1921 TO 1926.  THIS CALFUN ALSO GIVES THE COUNTS
C   ABSORBED BY ALPHA-FE AND THE TOTAL COUNTS ABSORBED. THIS VERSION
C   OF FIVECALF IS FOR 336 C DATA ONLY.
C
C
C           FIVECALF    22 NOV 80
C
C
C   THE REQUIRED VARIABLES ARE:
C
C      ONE VALUE OF H-FIELD FOR ALPHA IRON: X(1)
C
C      THREE VALUES OF H-FIELD FOR FE3B: X(2) TO X(4)
C
C      ONE VALUE OF TOTAL INTENSITY FOR ALPHA FE: X(5)
C
C      ONE VALUE OF TOTAL INTENSITY FOR FE3B: X(6)
C
C      THREE VALUES OF LINEWIDTH FOR FE3B: X(7) TO X(9)
C
C      ONE VALUE OF ISOMER SHIFT FOR ALPHA FE: X(10)
C
C      THREE VALUES OF ISOMER SHIFT FOR FE3B: X(11) TO X(13)
C
C      ONE VALUE OF TOTAL INTENSITY FOR THE FE3B2O: X(14)
C
C      BASELINE IS LAST VARIABLE: X(15)
C
C      TOTAL OF 15 VARIABLES REQUIRED
```

```
C
      COMMON W(13(??),XD(432),YD(432),F3(432),YDY(402),YCY(432),FSO(432),NBASE
      COMMON /HEADING/TITL(18)
      COMMON /NAM/XINIT(25),PRM(25),ERX(25),NBASE
      COMMON /CALF/ IFLAG
      DIMENSION F(4,2),X(25)
      REAL V(35),MUEX,MUGND,MUSUBN,LIGHT,H,B1(5)
C
      MUEX=.11491
      MUGND=-.19121E
      R=MUEX/(MUGND*3.)
C
C   FACTOR CONVERTS FROM ENERGY UNITS TO VELOCITY UNITS.
C
C                GZERO*MUSUBN*LIGHT*F1*F2
C       FACTOR = -----------------------
C                     2.*EZERO*F3
C
      GZERO=.18648
      MUSUBN=5.u5E-27
      LIGHT=2.99E11
      F1=1.8E3
      F2=1.0E-?
      EZERO=16.4125E3
      F3=1.5u2E-19
C
      FACTOR=(GZEFO*MUSUBN*LIGHT*F1*F2)/(EZERO*F3*2.)
C
C     ...FACTOR*(2.*R-1.)
C     ...FACTOR*( R-1.)
C     ...FACTOR*( R+1.)
C
      IF(IFLAG)25,25,19
C
C IF IFLAG IS NOT POSITIVE CALFUN IS BEING CALLED FOR PRINTING ONLY
```

```
C
10      CONTINUE
C
C       CALCULATE PEAK VELOCITIES FOR EACH SITE
C
        DO 11 I=1,9
11      X(I)=ABS(X(I))
C
C       THE FOLLOWING IS FOR THE ALPHA IRON SPECTRUM.
C       H IS THE HYPERFINE FIELD AND S IS THE ISOMER SHIFT.
C       V(1) TO V(6) ARE THE VELOCITIES OF PEAKS ONE TO SIX.
C
        H=X(1)
        S=X(10)
        V(1)=A*H+S
        V(2)=C*H+S
        V(3)=-C*H+S
        V(4)=C*H+S
        V(5)=-D*H+S
        V(6)=-A*H+S
C
C       THE FOLLOWING IS FOR THE FIRST FE33 SPECTRUM.
C
        H=V(2)
        S=X(11)
        Q=i.
        V(7)=A*H+S+Q
        V(13)=D*H+S-Q
        V(19)=-C*H+S-Q
        V(25)=C*H+S-Q
        V(14)=-D*H+S-Q
        V(8)=-A*H+S+Q
C
C       THE FOLLOWING IS FOR THE SECOND FE33 SPECTRUM.
C
        H=X(3)
```

```
      S=X(12)
      V(9)=A*H+S+Q
      V(15)=D*H+S-Q
      V(21)=-C*H+S-Q
      V(22)=C*H+S-Q
      V(16)=-D*H+S-Q
      V(10)=-A*H+S+Q
C
C     THE FOLLOWING IS THE THIRD FE3B SPECTRUM.
      H=X( )
      S=X(13)
      V(11)=A*H+S+Q
      V(17)=D*H+S-Q
      V(23)=-C*H+S-Q
      V(24)=C*H+S-Q
      V(18)=-D*H+S-Q
      V(12)=-A*H+S+Q
C
C     THE FOLLOWING IS THE FE8DR2Q GLASS SPECTRUM, IT MUST BE CHANGED
C     TO MATCH THE NON-CRYSTALLIZED GLASS SPECTRUM FOR A GIVEN
C     TEMPERATURE.
C
      H=145.
      S=.2..
      Q=-..05
      V(25)=A*H+S+Q
      V(26)=D*H+S-Q
      V(27)=-C*H+S-Q
      V(28)=C*H+S-Q
      V(29)=-D*H+S-Q
      V(30)=-A*H+S+Q
 26   CONTINUE
C
C     CALCULATE THE SPECTRUM
C
      AREE=0.0
      ATOT=0.0
      DO 30 I=1,NP
      IF(I.LE.150 .OR. I.GE.151) GO TO 31
```

51

```
      YC(I)=1-(..55*YD(I-1)+..95*YD(I+1)+.99*YD(I))/X(NBASE)
      GO TO 36
31    YC(I)=1.
      DO 37 K=1,30
      IF(K.EQ.1 .OR. K.EQ.6) TI=X(5)
      IF(K.EQ.2 .OR. K.EQ.5) TI=X(5)*2./3.
      IF(K.EQ.3 .OR. K.EQ.4) TI=X(5)/3.
      IF(K.GT.6 .AND. K.LT.13) TI=X(5)
      IF(K.GT.12 .AND. K.LT.19) TI=X(6)*X(7)*2./3./X(8)
      IF(K.GT.18) TI=X(6)+X(7)/3./X(9)
      IF(K.LT.7) B=(.56
      IF(K.GT.6 .AND. K.LT.13) B=X(7)
      IF(K.GT.12 .AND. K.LT.19) B=X(8)
      IF(K.GT.18 .AND. K.LT.25) B=X(9)
      IF(K.LT.24) GO TO 32
      YCP=TI/((((XD(I)-V(K))**2*4.)/B**2)+1.)
      GO TO 37
32    TI1=ABS(X(14))
C
C  THE FOLLOWING ARE THE LINEWIDTHS OF THE SIX GLASS PEAKS.
C
      B1(1)=2.45
      B1(2)=1.640
      B1(3)=1.39
      B1(4)=1.25
      B1(5)=1.76
      B1(6)=2.59
      IF(K.EQ.25) TI=TI1
C
C  THE 1.36 IN THE FIRST AND FOURTH LINES FOLLOWING IS THE
C  INTENSITY RATIO OF PEAK 2 TO PEAK 1 (OF THE GLASS).
C
      IF(K.EQ.26) TI=TI1*1.36*B1(1)/B1(2)
      IF(K.EQ.27) TI=TI1*B1(1)/3./B1(3)
      IF(K.EQ.28) TI=TI1*B1(1)/3./B1(4)
      IF(K.EQ.29) TI=TI1*1.36*B1(1)/B1(5)
      IF(K.EQ.30) TI=TI1*B1(1)/B1(6)
      YYY=(XD(I)-V(K))**2/.3667/B1(K-24)**2
      IF(YYY.GT.160.) YYY=160.
```

```
      YCP=(TI/SQRT(1.133*31(K-24)**2))*EXP(-YYY)
C
C     CALCULATE COUNTS ABSORBED BY ALPHA-FE.
C
 33   IF(K.LT.7) AAFE=AAFE+YCP
 35   YC(I)=YC(I)+YCP
C
C     CALCULATE TOTAL COUNTS ABSORBED.
C
 36   ATOT=ATOT+YC(I)
      YC(I)=(1.0-YC(I))*X(NBASE)
 30   F(I)=(YD(I)-YC(I))/SQRT(YD(I))
      RETURN
C
C     ON THE FINAL CALL OF CALFUN PRINT THE PEAK VELOCITIES AND
C     THE COUNTS ABSORBED.
C
 25   CONTINUE
      PRINT 92
 92   FORMAT(1H1,//,38H THE PEAK VELOCITIES ARE (IN MM/SEC):,//)
      PRINT 10,(V(I),I=1,6)
      PRINT 93
 93   FORMAT(//,53H THE PEAK VELOCITIES FOR THE THREE FE33 SPECTRA ARE:
     1,//)
      DO 85 I=7,11,2
      PRINT 10,V(I),V(I+5),V(I+12),V(I+13),V(I+7),V(I+1)
 85   PRINT 90
      PRINT 94,AAFE
 94   FORMAT(////,63H THE TOTAL ALPHA IRON AREA (SIX PEAKS) IS:,//,
     1F10.4,//)
      PRINT 95,ATOT
 95   FORMAT(//,37H THE AREA UNDER THE ENTIRE CURVE IS:,//,F10.4)
      PRINT 90
 96   FORMAT(1H1)
 90   FORMAT(/)
 100  FORMAT(5X,7F10.4)
      RETURN
      END
```

```
      SUBROUTINE CALFUN(NP,NPAR,F,X)
C  THIS CALFUN FITS ONLY PEAKS ONE AND SIX OF THE ALPHA-FE SPECTRUM.
C  IT ADDS A GAUSSIAN SHAPED BACKGROUND TO THE ALPHA-FE TO ACCOUNT FOR
C  THE CLOSENESS OF THE GLASS SPECTRUM TO THE CRYSTALLIZED ALPHA-FE
C  SPECTRUM.  IT FITS THE CENTER PORTION OF THE SPECTRUM WITH THE
C  APPROXIMATE DATA VALUES.
C
C              ALPHA-BG   22 OCT 80
C
C  THE REQUIRED VARIABLES ARE:
C
C  ONE VALUE OF H-FIELD FOR ALPHA IRON: X(1)
C
C  ONE VALUE OF H-FIELD FOR THE BACKGROUND CURVE: X(2)
C
C  ONE VALUE OF ISOMER SHIFT FOR ALPHA IRON: X(3)
C
C  ONE VALUE OF ISOMER SHIFT FOR THE BACKGROUND CURVE: X(4)
C
C  TWO VALUES OF LINE WIDTH: X(5) TO X(6)
C
C  ONE VALUE OF TOTAL INTENSITY OF PEAK 1: X(7)
C       FOR ALPHA IRON
C
C  ONE VALUE OF TOTAL INTENSITY OF THE BACKGROUND: X(8)
C
C  BASELINE IS LAST VARIABLE: X(9)
C
C  TOTAL OF 9 VARIABLES REQUIRED
C
      COMMON W(13000),XD(402),YD(402),Y2(402),YDY(402),YCY(402),FSD(402),NBASE
      COMMON /HEADING/TITL(18)
      COMMON /NAM/XINIT(25),PRM(25),ERX(25),NBASE
```

```
      COMMON /CALF/ IFLAG
      DIMENSION F(4,12),X(25)
      REAL V(6),MUEX,MUGND,MUSUBN,LIGHT

C     LOAD VALUES OF BINOMIAL PROBABILITIES

      MUEX=.15491
      MUGND=-.09.28E
      R=MUEX/(MUGND*3.)

C     FACTOR CONVERTS FROM ENERGY UNITS TO VELOCITY UNITS.

C                 GZERO*MUSUBN*LIGHT*F1*F2
C     FACTOR = --------------------------------
C                      2.*EZERO*F3

      GZERO=.18448
      MUSUBN=5.05E-27
      LIGHT=2.998E11
      F1=1.9E3
      F2=1.4E-4
      EZERO=14.4125E3
      F3=1.602E-15

      FACTOR=(GZERO*MUSUBN*LIGHT*F1*F2)/(EZERO*F3*2.)

      A = FACTOR*(3.*R-1.)
      D = FACTOR*( R-1.)
      C = FACTOR*( R+1.)

      IF(IFLAG)25,25,10

C     IF IFLAG IS NOT POSITIVE CALFUN IS BEING CALLED FOR PRINTING ONLY

10    CONTINUE
C
```

55

```
C     CALCULATE PEAK VELOCITIES FOR EACH SITE
C
      DO 11 I=1,2
      X(I)=ABS(X(I))
11    V(1)=A*X(1)+X(3)
      V(2)=A*X(2)+X(4)
      V(3)=-A*X(2)+X(4)
      V(4)=-A*X(1)+X(3)
      DO 33 I=5,8
33    Y(I)=ABS(X(I))
25    CONTINUE
C
C     CALCULATE THE SPECTRUM
C
      AAFE=0.0
      ATOT=0.0
      DO 31 I=1,NP
      IF(I.LT.132 .OR. I.GT.214) GO TO 31
      YD(I)=1-(.065*YD(I-1)+.065*YD(I+1)+.39*YD(I))/X(NBASE)
      GO TO 36
31    YC(I)=0.
      DO 35 K=1,4
      IF(K.EQ.1 .OR. K.EQ.4) TI=X(7)
      IF(K.EQ.2 .OR. K.EQ.3) TI=X(8)
      IF(K.EQ.2 .OR. K.EQ.3.) GO TO 32
      YCP=TI/((((XD(I)-V(K))**2+4.)/X(5)**2)+1.)
      AAFE=AAFE+YCP
      GO TO 35
32    YYY=(XD(I)-V(K))**2/(2.*(.42.7*X(5))**2)
      IF(YY.GT.10.) YYY=10.
      YCP=TI/SQRT(6.2830)/.4247/X(5)*EXP(-YYY)
35    YC(I)=YC(I)+YCP
36    ATOT=ATOT+YC(I)
30    YC(I)=(1.5-YC(I))*X(NBASE)
      F(I)=(YD(I)-YC(I))/SQRT(YD(I))
      RETURN
C
C     ON THE FINAL CALL OF CALFUN PRINT THE PEAK VELOCITIES
C
26    CONTINUE
```

```
      PRINT 9C
      PRINT*,::
      PRINT*,:: THE PEAK VELOCITIES   ARE:"
      PRINT*,::
      PRINT 1CC,(V(I),I=1,4)
      PRINT*,::
      PRINT*,::
      PRINT*,"THE AREA UNDER PEAKS 1 AND 5 OF ALPHA IRON IS: ",AAFE
      PRINT*,:: THE TOTAL ALPHA IRON AREA IS TWICE THAT AREA."
      PRINT*,::
      PRINT*,"THE AREA UNDER THE ENTIRE CURVE IS: ",ATOT
      PRINT*,::
      PRINT 9C
  9C  FORMAT(1H1)
  1CC FORMAT(5X,7F1C.4)
      RETURN
      END
```

57

APPENDIX D

GENFIT Instructions

This appendix contains instructions for using GENFIT
with one of the three CALFUNs listed in Appendices A, B, and
C. It is presented in two parts; the first explains the con-
trol cards and parameters used when running GENFIT, the
second describes how to alter FIVECALF for different tempera-
ture runs.

Control Deck

The following control deck precedes the data. It permits
processing on the AFIT terminal only.

```
DEB,T300,CM120000,STCSB. M799999,DBELLER,4369.
ATTACH,A,GENFIT,MR=1
FIN,I=A,OPT=0,R=2,L=0.
ATTACH,COMPILE,GAUSSCALF,MR=1
FIN,I,OPT=0,R=2,L=0.
ATTACH,P,CCPLOT56X,ID=LIBRARY,SN=ASD.
LIBRARY,P.
LDSET,PRESET=ZERO
LGO.
7/8/9
```

The first two cards of the data deck are title cards. They
are used to identify the material and run number, and the
CALFUN used for processing the data. The third data card con-
tains processing parameters as explained below.

58

```
FEB1(11/15)80. 611 X.
FIVECALI
12,188,218,2,1,200,0.
```
— includes baseline as a variable parameter

— maximum calls of CALFUN

— type of plot

— number of times timing channels have exceeded one million counts

{ GENFIT does not fit the velocity curve

between these channel numbers

— number of variable parameters in the attached CALFUN

The parameter cards then follow this card. In this case, there are twelve (as in above card). Two are given for example (format I6, open):

```
  HFIELD      310.
     .
     .
     .
     .
     .
  BASELN      52000
```

The Mossbauer data deck follows immediately after the parameter cards. There are forty data cards, in I3, 10I7 format. They contain the channel number of the first data entry on each card plus 10 channels of data. The final two cards contain more processing parameters.

`1. , .,21,60,550,505,0`

- number of times the data is smoothed before processing
- range of channels of right-hand zone for polynomial baseline fitting
- range of channels of left-hand zone for polynomial baseline fitting
- number of zones to be used for baseline fitting
- number of times baseline has exceeded one million counts
- order of the polynomial fit to the baseline

9.0,2.25

- distance between hack marks on the horizontal (velocity) scale of the CALCOMP plot, in mm/sec
- horizontal scale distance (-9 to +9 mm/sec)

The final card for processing Mossbauer data is the end-of-job card:

6/7/8/9 END OF JOB

Altering FIVECALF

FIVECALF must be changed for different temperature runs because the glass spectrum changes over a given temperature range. The average hyperfine field, the distribution of fields, the relative intensity of peak two to peak one, and the isomer shift and quadrupole split all vary with temperature. Altering FIVECALF is rather simple, however. Once GAUSSCALF has been run with a non-crystallized spectrum and the parameters

60

obtained, the necessary changes to FIVECALF can be made.

They are listed below by line number in Appendix B.

000220   change temperature to that which this copy of FIVECALF
        will be for

001460   change H=145. to the hyperfine field obtained with
        GAUSSCALF

001470   change S=-.200 to the isomer shift obtained

001480   change Q=-.005 to the quadrupole split obtained

001840   change B1(1) to the value obtained for the linewidth
        of peak one

001850   change B1(2) to the value obtained for the linewidth
        of peak two

001860   change B1(3) to the value obtained for the linewidth
        of peak three

001870   change B1(4) to the value obtained for the linewidth
        of peak four

001880   change B1(5) to the value obtained for the linewidth
        of peak five

001890   change B1(6) to the value obtained for the linewidth
        of peak six

001950   change 1.30 to the value of the ratio of peak two to
        peak one

001980   change 1.30 to the value of the ratio of peak two to
        peak one

APPENDIX E

Applications of Metallic Glasses

In this appendix some of the existing and proposed
applications of the metallic glasses are described. The
mechanical, electrical, and magnetic properties of some of
the glasses make them suitable for many uses. Two commercial
applications have existed since 1976. A woven fabric has been
manufactured for use as magnetic shielding. It performs as
well as $Fe_{80}Ni_{20}$ foil, and it has the advantage of high flexi-
bility. The other current application of metallic glass is
in magnetostrictive delay lines, which take advantage of the
large magnetostriction of the metallic glasses and the high
change in Young's modulus with applied magnetic field. Other
uses are envisioned which take advantage of various combina-
tions of magnetic "softness," mechanical hardness, and high
electrical resistivity.

Due to the ease of reversing magnetic fields in the
metallic glasses, power transformers with these materials
in their cores would lose much less energy to heating. These
glassy metals have been proposed for winding the cores of
inversion transformers, current and pulse transformers, and
magnetic amplifiers. They also are likely candidates for the
"read" and "write" heads in magnetic tape recorders and disc

62

systems. Their electrical resistance properties make them suitable for electrical resistors, low temperature heating wires, and resistance thermometers.

The various mechanical properties of the glassy metals make them useful for many other applications. Because of high tensile strength, some of the glasses might be used as reinforcing filaments in tires, transmission belts, or high pressure tubing; or as stress transducers in a multi-vibrator configuration. Their corrosion resistance makes them useful in underwater cables or biomaterials. The hardness and ability to be sharpened make some of the glassy metals suitable materials for manufacturing cutting devices.

Besides the above applications which are based on the macro-properties of the metallic glasses, there is at least one use based on their micro-structure: they have been proposed as the storage medium for magnetic "bubble" memory systems. Since the bubbles in the metallic glasses are one-fifth the size of those in synthetic garnet, the storage density would be 25 times greater. The vortices (important in superconductors) are 10 times smaller. If these can be used for storage, the information density could be 250 times greater than that now projected in synthetic garnet bubble memory systems.

All of the above applications can take advantage of two common properties of the metallic glasses: they are very easy to work with, due to their flexible-fiber form; and they are inexpensive to manufacture, due to the one-step production

proce... with no subsequent treatments necessary. A few of
the authors who have researched the applications of the
metallic glasses--and will probably continue--are: C.D.
Graham, T. Egami, J.J. Gilman, P. Chaudhari, and F.E. Luborsky.

Vita

Denis Eugene Beller was born on November 22, 1950, in Okmulgee, Oklahoma, and is the son of Ernest E. and Ezma I. Beller. He graduated from Norte Del Rio High School in Sacramento, California in June 1968. He attended the University of Nevada and American River College before enlisting in the Air Force in 1971. In May 1976 he graduated with honors from the University of Colorado with a degree of Bachelor of Science in Chemical Engineering. Following graduation from Air Force Officer Training School, he served as a test engineer at the Air Force Rocket Propulsion Laboratory, Edwards AFB, California. Prior to attending the Air Force Institute of Technology, he served as a test section chief and senior test engineer at Edwards. He and his wife Judy have two sons.

Permanent Address: 2101 Middleberry Rd.
Sacramento, Ca. 95815

REPORT DOCUMENTATION PAGE	READ INSTRUCTIONS BEFORE COMPLETING FORM

1 REPORT NUMBER	2 GOVT ACCESSION NO.	3 RECIPIENT'S CATALOG NUMBER
AFIT/GNE/PH/81M-1	AD-A100 818	

4 TITLE (and Subtitle)	5 TYPE OF REPORT & PERIOD COVERED
CRYSTALLIZATION KINETICS OF TWO METALLIC GLASSES BY MOSSBAUER SPECTROSCOPY	MS Thesis
	6 PERFORMING ORG REPORT NUMBER

7 AUTHOR(s)	8 CONTRACT OR GRANT NUMBER(s)
Denis L. Beller Captain, USAF	

9 PERFORMING ORGANIZATION NAME AND ADDRESS	10 PROGRAM ELEMENT PROJECT TASK AREA & WORK UNIT NUMBERS
Air Force Institute of Technology (AFIT/EN) Wright-Patterson AFB, Ohio 45433	

11 CONTROLLING OFFICE NAME AND ADDRESS	12 REPORT DATE
	7 March 1981
	13 NUMBER OF PAGES
	75

14 MONITORING AGENCY NAME & ADDRESS(if different from Controlling Office)	15 SECURITY CLASS. (of this report)
	UNCLASSIFIED
	15a. DECLASSIFICATION DOWNGRADING SCHEDULE

16 DISTRIBUTION STATEMENT (of this Report)

Approved for public release; distribution unlimited.

17 DISTRIBUTION STATEMENT (of the abstract entered in Block 20, if different from Report)

APPROVED FOR PUBLIC RELEASE AFR 1

1981 JUN 11

18 SUPPLEMENTARY NOTES

APPROVED RELEASE AFR 190-17

Fredric C. Lynch

FREDRIC C. LYNCH, Major, USAF
Director of Public Affairs
Air Force Institute of Technology (ATC)
Wright-Patterson AFB, OH 45433

19 KEY WORDS (Continue on reverse side if necessary and identify by block number)

Metallic Glasses   Crystallication Kinetics
Aging Kinetics   Mossbauer Spectroscopy
$Fe_{80}B_{20}$

20 ABSTRACT (Continue on reverse side if necessary and identify by block number)

In this study, Mossbauer spectroscopy was used to examine thermal aging of two metallic glasses. $Fe_{80}B_{20}$ was isothermally annealed at 573, 604, 611, and 626 K and $Fe_{80}P_{6.5}C_{3.5}B_{10}$ was annealed at 614, 716, and 744 K. The activation energy of $Fe_{80}B_{20}$, determined from the growth of —>

DD FORM 1473 1 JAN 73   EDITION OF 1 NOV 65 IS OBSOLETE

Block 20:

α-Fe crystals, was 0.256 ± 0.006 MJ/mole. The projected lifetime of this glass, based on the onset of crystallization, is 400 years. No quantitative data were obtained for $Fe_{80}P_{6.5}C_{3.5}B_{10}$; however, based on the higher temperature required for crystallization, it is expected to have a longer lifetime.

END

DATE
FILMED

7-81

DTIC